Spatial patterns of ectoenzymatic kinetics in relation to biogeochemical properties in the Mediterranean Sea and the concentration of the fluorogenic substrate used

France van Wambeke, Elvira Pulido-Villena, Philippe Catala, Julie Dinasquet, Kahina Djaoudi, Anja Engel, Marc Garel, Sophie Guasco, Barbara Marie, Sandra Nunige, et al.

▶ **To cite this version:**

France van Wambeke, Elvira Pulido-Villena, Philippe Catala, Julie Dinasquet, Kahina Djaoudi, et al.. Spatial patterns of ectoenzymatic kinetics in relation to biogeochemical properties in the Mediterranean Sea and the concentration of the fluorogenic substrate used. Biogeosciences, 2021, 18 (7), pp.2301-2323. 10.5194/bg-18-2301-2021 . hal-03195714

HAL Id: hal-03195714
https://amu.hal.science/hal-03195714v1

Submitted on 12 Apr 2021

HAL is a multi-disciplinary open access archive for the deposit and dissemination of scientific research documents, whether they are published or not. The documents may come from teaching and research institutions in France or abroad, or from public or private research centers.

L'archive ouverte pluridisciplinaire **HAL**, est destinée au dépôt et à la diffusion de documents scientifiques de niveau recherche, publiés ou non, émanant des établissements d'enseignement et de recherche français ou étrangers, des laboratoires publics ou privés.

Distributed under a Creative Commons Attribution - NoDerivatives 4.0 International License

Biogeosciences, 18, 2301–2323, 2021
https://doi.org/10.5194/bg-18-2301-2021
© Author(s) 2021. This work is distributed under
the Creative Commons Attribution 4.0 License.

Biogeosciences Open Access EGU

Spatial patterns of ectoenzymatic kinetics in relation to biogeochemical properties in the Mediterranean Sea and the concentration of the fluorogenic substrate used

France Van Wambeke[1], Elvira Pulido[1], Philippe Catala[3], Julie Dinasquet[2,3], Kahina Djaoudi[1,4], Anja Engel[5], Marc Garel[1], Sophie Guasco[1], Barbara Marie[3], Sandra Nunige[1], Vincent Taillandier[6], Birthe Zäncker[6,7], and Christian Tamburini[1]

[1]Aix-Marseille Université, CNRS/INSU, Université de Toulon, IRD, Mediterranean Institute of Oceanography (MIO) UM110, 13288, Marseille, France
[2]Marine Biology Research Division, Scripps Institution of Oceanography, UCSD, La Jolla, CA, USA
[3]Sorbonne Universités, UPMC University Paris 6, Laboratoire d'Océanographie Microbienne (LOMIC), Observatoire Océanologique, 66650, Banyuls/mer, France
[4]Molecular and Cellular Biology, The University of Arizona, Tucson, AZ, USA
[5]GEOMAR, Helmholtz Centre for Ocean Research, Kiel, Germany
[6]CNRS, Sorbonne Universités, Laboratoire d'Océanographie de Villefranche (LOV), UMR7093, 06230 Villefranche-sur-Mer, France
[7]The Marine Biological Association of the UK, Plymouth, United Kingdom

Correspondence: France Van Wambeke (france.van-wambeke@mio.osupytheas.fr)

Received: 1 July 2020 – Discussion started: 17 August 2020
Revised: 15 February 2021 – Accepted: 24 February 2021 – Published: 9 April 2021

Abstract. Ectoenzymatic activity, prokaryotic heterotrophic abundances and production were determined in the Mediterranean Sea. Sampling was carried out in the sub-surface, the deep chlorophyll maximum layer (DCM), the core of the Levantine intermediate waters and in the deeper part of the mesopelagic layers. Michaelis–Menten kinetics were assessed using a large range of concentrations of fluorogenic substrates (0.025 to 50 µM). As a consequence, Km (Michaelis–Menten half-saturation constant) and Vm (maximum hydrolysis velocity) parameters were determined for both low- and high-affinity enzymes for alkaline phosphatase, aminopeptidase (LAP) and β-glucosidase (βGLU). Based on the constant derived from the high-LAP-affinity enzyme (0.025–1 µM substrate concentration range), in situ hydrolysis of N proteins contributed 48 % ± 30 % to the heterotrophic bacterial nitrogen demand within the epipelagic layers and 180 % ± 154 % in the Levantine intermediate waters and the upper part of the mesopelagic layers. The LAP hydrolysis rate was higher than bacterial N demand only within the deeper layer and only when considering the high-affinity enzyme. Based on a 10 % bacterial growth efficiency, the cumulative hydrolysis rates of C proteins and C polysaccharides contributed on average 2.5 % ± 1.3 % to the heterotrophic bacterial carbon demand in the epipelagic layers sampled (sub-surface and DCM). This study clearly reveals potential biases in current and past interpretations of the kinetic parameters for the three enzymes tested based on the fluorogenic-substrate concentration used. In particular, the LAP / βGLU enzymatic ratios and some of the depth-related trends differed between the use of high and low concentrations of fluorogenic substrates.

1 Introduction

In aquatic environments, the organic matter compounds available for bacterial utilization are dominated by polymeric material (Simon et al., 2002; Aluwihare et al., 1997). In order to be assimilated, first they need to be hydrolyzed into smaller molecules by ectoenzymes. This represents a lim-

iting step in organic matter degradation and in nutrient regeneration (Hoppe, 1983; Chróst, 1991). Whether the ectoenzymatic activity should be considered to be limiting the rate of organic matter remineralization is a subject of debate since hydrolysis and consumption of the by-products of hydrolysis are not always coupled (Smith et al., 1992). Bacterial ectoenzymatic hydrolysis is usually determined using fluorogenic substrates (Hoppe, 1983), which, when cleaved by the ectoenzyme, triggers the release of a fluorescent by-product. The fluorescence increase is monitored over time, thus allowing the determination of the hydrolysis rate. Kinetic experiments are time-consuming, and most studies reporting ectoenzymatic activity examined enzyme kinetic patterns using one or two samples. A single, presumably saturating substrate concentration is then used to determine the activity of all the samples. Baltar et al. (2009b) cite 17 published studies on ectoenzymatic activity, of which 12 used a single substrate concentration, ranging from 0.02–1000 µM (with a median of 50 µM). Only five studies used a range of substrate concentrations to determine enzyme kinetics. In these five studies the lowest substrate concentration used was 50 nM (typically the lower concentration in the set is between 1 and 5 µM), while the highest concentration was 1200 µM (the range of the higher concentrations in the set is 5–1200 µM, with a median of 200 µM). Another compilation of data from the Mediterranean Sea (Zaccone and Caruso, 2019) showed that 6 out of 22 studies used a single concentration (assumed to be saturating) with a median of 125 µM for leucine 7-amido–4-methyl coumarin and 50 µM for methylumbelliferyl–phosphate. Likewise, the remaining studies assessed enzyme kinetics with a highly variable range of substrate concentrations (lowest concentrations of 0.025–200 µM, with a median of 0.1 µM; highest concentrations of 1–4000 µM, with a median of 20 µM). However, the combination of (i) non-specificity in the enzymes, (ii) the heterogeneity of enzymatic systems within single species, (iii) the diversity in species present, and (iv) the range and variability in concentrations of surrounding substrates will result in multiphasic kinetics (Chróst, 1991; Arnosti, 2011; Sinsabaugh and Follstad Shah, 2012, and references therein). Ectoenzymes are produced by a diversity of microorganisms. Their activity depends on a patchy distribution of natural substrates and a variety of natural (potentially unknown) molecules which can be hydrolyzed by the same enzymes, with potentially different affinities. For instance, cell-specific activities and types of activities were shown to be very variable among 44 heterotrophic bacterial strains isolated from the Californian coast and experimental phytoplankton blooms, both from particles and in the suspended phase (Martinez et al., 1996). Arrieta and Herndl (2001) showed differences in Km (Michaelis–Menten half-saturation constant) and Vm (maximum hydrolysis velocity) in an assessment of the diversity of marine bacterial β-glucosidases taken from a natural community. In the water column, different kinetic systems were also observed, which were generally attributed to attached or free-living bacteria having different affinities for substrates: *k*-strategist oligotrophic bacteria (with both low Km and Vm) or *r*-strategist copiotrophic bacteria (with both high Km and Vm; Koch, 2001). At depth, the combination of refractory dissolved organic matter (DOM) with recent and freshly sinking particles would promote multiphasic kinetics for ectoenzymatic activity. Biphasic kinetic systems have been described in areas where increasing gradients of polymeric material are expected due to the high concentration of particles, e.g., near the bottom and sediments for aminopeptidase (Tholosan et al., 1999) and in a shallow bay for phosphatases (Bogé et al., 2013). Most studies have shown that cell-specific ectoenzymatic activities on aggregates are $\sim$ 10-fold higher than those of the surrounding assemblages (for example during a decaying bloom; Martinez et al., 1996). Biphasic kinetics were also attributed to free-living bacteria versus attached heterotrophic bacteria, the latter adapted to high substrate concentrations (with both higher Vm and Km; Unanue et al., 1999). Size fractionation is commonly carried out prior to incubation with fluorogenic substrates in order to determine the size fraction in which the activity is dominant. However, size fractionation prior to incubation biases ectoenzymatic activities due to filtration artifacts and the disruption of trophic relationships between primary producers, heterotrophic bacteria, protozoans and particulate matter. Despite such biases, carbon budgets have shown that the prokaryotes attached to aggregates are a likely source of by-products for free-living prokaryotes (Smith et al., 1992). Measurements in bulk samples enable different enzymatic kinetics to be determined without disturbing relationships between free and attached prokaryotes and interactions between DOM and particulate organic matter (POM) during the incubations.

In the Mediterranean Sea, elemental C/N/P ratios of dissolved nutrients and organic matter are the subject of particular interest to elucidate the impact of P deficiency on DOC (dissolved organic carbon) accumulation in surface waters (Thingstad and Rassoulzadegan, 1995; Krom et al., 2004) given that the export of organic carbon in dissolved vs. particulate forms is linked to the P limitation in surface layers (Guyennon et al., 2015). Since the epipelagic layers are P- or N–P-limited during most of the stratification period, ectoenzymes such as phosphatase and aminopeptidase providing P and N sources from organic matter have been intensively studied as indicators of these limitations (Sala et al., 2001; Van Wambeke et al., 2002). However, the potential bias introduced by multiple kinetics when comparing different types of ectoenzymes and using a variable range of substrates is still poorly understood.

In this study, we investigated the Michaelis–Menten kinetics of three series of enzymes targeting proteins, phosphomonoesters and carbohydrates (leucine aminopeptidase, alkaline phosphatase and β-*D*-glucosidase, respectively) in the Mediterranean Sea. A wide range of substrate concentrations were tested to evaluate potential multiphasic kinetics.

Our aim was to evaluate potential biases in the interpretation of past and current enzymatic kinetics based on studies measuring rates with a reduced range of substrate concentrations or with the use of too high substrate concentrations. We also studied the links between ectoenzyme activities with the spatial (vertical and horizontal) trends in the quality of the available organic matter. In the Mediterranean Sea, the distribution of biogeochemical properties below the productive zone is the result of large-scale dynamic transport systems associated with three distinct thermohaline circulation cells (Wust, 1961; Hopkins, 1978; The Mermex Group, 2011, and references therein). These open cells convey fresh and cool waters of Atlantic origin to the upper 150–200 m water layer extending into the eastern part of the Levantine Sea. The return branch is composed of warm, saline waters – the Levantine intermediate water (LIW) – which spread over the whole Mediterranean Sea at depths of 200–500 m (Kress et al., 2003; Malanotte-Rizzoli et al., 2003; Schroeder et al., 2020). In addition, two closed cells, within each Mediterranean sub-basin, are driven by deep-water convection and spread below the LIW (e.g., Lascaratos et al., 1999; Testor et al., 2018).

This study focuses on the open waters of the Mediterranean Sea, examining four water layers: surface (generally P- or N-limited in stratification period), the deep chlorophyll maximum layer (coinciding with nutricline depths), the LIW and the deep waters. Alongside marine biogeochemical fluxes, atmospheric fluxes were quantified simultaneously during the same cruise. As a result of these exceptional simultaneous measurements, the data used in this paper are also used in another article of this special issue (Van Wambeke et al., 2020), where biogeochemical fluxes within the mixed layers are compared to wet- and dry-N and wet- and dry-P atmospheric fluxes.

2 Materials and methods

2.1 Sampling strategy

The PEACETIME cruise (https://doi.org/10.17600/17000300, Guieu and Desboeufs, 2017) was conducted from May to June 2017 along a transect extending from the western Mediterranean Basin to the center of the Ionian Sea (Fig. 1). For details on the cruise strategy, see Guieu et al. (2020a). Stations of short duration (< 8 h, 15 stations named SD1 to SD10; Fig. 1) and long duration (5 d, three stations named TYR, ION and FAST) were sampled. At least three casts were conducted at each short station. One focused on the first 250 m and the second one on the whole water column. These two casts were sampled with a standard CTD (conductivity–temperature–depth) rosette equipped with 24 Niskin bottles (12 L) and a Sea-Bird SBE9 underwater unit equipped with pressure, temperature (SBE3), conductivity (SBE4), chlorophyll fluorescence (Chelsea Acquatracka) and oxygen (SBE43) sensors. The third cast (from the surface to the bottom) was carried out using a trace-metal-clean (TMC) rosette mounted on a Kevlar cable and equipped with Go-Flo bottles that were sampled in a dedicated trace-metal-free container. The long stations situated in the center of the Tyrrhenian Sea (TYR), in the center of the Ionian Sea (ION) and in the western Algerian Basin (FAST) were selected using satellite imagery, altimetry and Lagrangian diagnostics to target dust deposition events (Guieu et al., 2020a). At these stations, repeated casts were performed, alternating CTD and TMC rosettes.

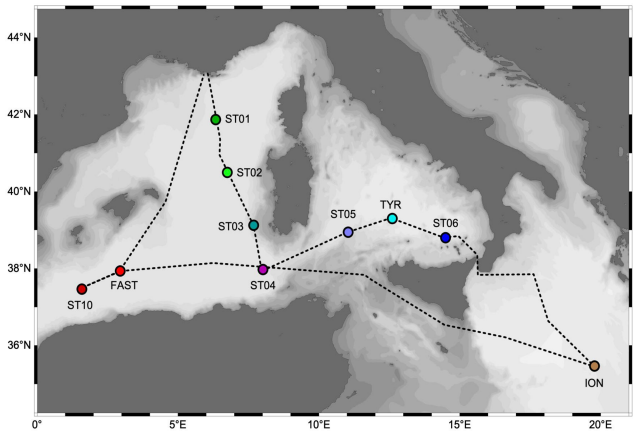

Figure 1. Sampling sites. Color codes on dots correspond to the plots in Fig. 2.

The water sampled with the conventional CTD rosette was used for measurements of heterotrophic bacterial production (BP; sensus stricto referring to heterotrophic prokaryotic production), heterotrophic bacterial abundance (BA; sensus stricto referring to heterotrophic prokaryotic abundances), ectoenzymatic activities (EEAs), chlorophyll stocks, particulate organic carbon (POC), nitrogen (PON), phosphorus (POP) and dissolved organic carbon (DOC). Dissolved inorganic nitrogen (DIN) and phosphorus (DIP) as well as dissolved organic nitrogen (DON) and phosphorus (DOP) were measured in samples collected using the TMC rosette

Details on sampling and analysis for the additional parameters presented in this paper (hydrographic properties, total chlorophyll *a* (Tchl *a*) are available in Taillandier et al. (2020), Guieu et al. (2020a) and Marañón et al. (2021) in this issue.

We focused on four layers of the water column: two in epipelagic waters (at 5 m near the surface (SURF) and in the deep chlorophyll maximum layer (DCM), localized by the in vivo fluorescence measured continuously during downcasts) and two in deeper layers (in the LIW characterized by a sub-surface salinity maximum and oxygen minimum during downcasts (LIW) and at 1000 m, the limit between mesopelagic water and bathypelagic water (MDW), except

at FAST and ION, where the MDW samples were collected at 2500 and 3000 m, respectively (Table 1)).

2.2 Biochemistry

Nitrate (NO_3), nitrite (NO_2) and orthophosphate (DIP) concentrations were determined using a segmented-flow autoanalyzer (AAIII HR Seal Analytical) according to Aminot and Kérouel (2007). The quantification limits were 0.05 µM for NO_3, 0.01 µM for NO_2 and 0.02 µM for DIP. DON and DOP were determined after high-temperature (120 °C) persulfate wet oxidation (Raimbault et al., 1999) as follows: the water sample was filtered through a 0.2 µm polyethersulfone (PES) membrane and collected into 25 mL glass flasks. Samples were immediately poisoned with 100 µL H_2SO_4 5 N and stored in the dark until analysis in the laboratory. Samples (20 mL) were then transferred in Teflon vials for wet oxidation. Nitrate and phosphate formed corresponding to the total N and P in the dissolved pool (TDN and TDP) were determined as described for dissolved inorganic nutrients. DON and DOP were obtained from the difference between TDN and DIN and TDP and DIP, respectively. The limits of quantification were 0.5 and 0.02 µM for DON and DOP, respectively.

Particulate organic nitrogen and phosphate (PON, POP) were determined using the same wet-oxidation method (Raimbault et al., 1999). Samples (1.2 L) were collected into polycarbonate bottles and filtered through pre-combusted (450 °C, 4 h) glass fiber filters (Whatman 47 mm GF/F). Filters were stored at −20 °C until analysis. In the laboratory, samples were placed in Teflon vials with 20 mL of ultrapure water (Milli-Q grade) and 2.5 mL of the wet-oxidation reagent for mineralization. The nitrate and orthophosphate produced were analyzed as described previously. The limits of quantification were 0.02 and 0.001 µM for PON and POP, respectively.

In epipelagic samples from nutrient-depleted layers, DIP and NO_3 were determined using the liquid waveguide capillary cell (LWCC) method (Zhang and Chi, 2002) with enhanced sensitivity of the spectrophotometric measurement by an increase in the length of the optical path of the measurement cell to 2.5 m. For DIP, the detection limit was 0.8 nM, and the response was linear up to about 150 nM; for NO_3, the detection limit was 6 nM. Phosphacline and nitracline depths were determined as the layers where 50 nM concentration is reached.

Samples for dissolved organic carbon (DOC) were filtered through two pre-combusted (24 h, 450 °C) glass fiber filters (Whatman GF/F, 25 mm) using a custom-made glass and Teflon filtration syringe system. Samples (10 mL in duplicates) were collected into pre-combusted glass ampoules and acidified to pH 2 with phosphoric acid (H_3PO_4). Ampoules were immediately sealed and stored in the dark at room temperature. Samples were analyzed by high-temperature catalytic oxidation (HTCO) on a Shimadzu total organic carbon analyzer (TOC-L-CSH; Cauwet, 1999). Prior to injection, DOC samples were purged with CO_2-free air for 6 min to remove inorganic carbon. A total of 100 µL of samples were injected in triplicate, and the analytical precision was 2 %. Consensus reference materials (https://hansell-lab.rsmas.miami.edu/consensus-reference-material/index.html, last access: 29 March 2021) were injected every 12 to 17 samples to ensure stable operating conditions. The nominal and measured DOC concentrations of the two batches used in this study were 42–45 and 43–45 µM, respectively, for batch 14-2014#07-14 and 42–44 and 42–49 µM, respectively, for batch 17-2017#04-17. Particulate organic carbon (POC) was measured using a CHN analyzer using the improved analysis proposed by Sharp (1974).

Samples (20 mL) for total hydrolyzable carbohydrates (TCHOs) > 1 kDa were collected into pre-combusted glass vials (8 h at 500 °C) and stored at −20 °C until analysis. Samples were desalinated using membrane dialysis (1 kDa molecular weight cut-off (MWCO), Spectra Por) at 1 °C for 5 h. Samples were then hydrolyzed for 20 h at 100 °C with 0.8 M HCl final concentration with subsequent neutralization using acid evaporation (N_2, for 5 h at 50 °C). TCHOs were analyzed using high-performance anion exchange chromatography with pulsed amperometric detection (HPAEC–PAD), which was applied on a Dionex ICS 3000 ion chromatography system (Engel and Händel, 2011). Two replicates for each TCHO sample were analyzed.

Total hydrolyzable amino acids (TAAs) were determined from a 5 mL water sample collected into pre-combusted glass vials (8 h, 500 °C) and stored at −20 °C. Samples were measured in duplicates. The samples were hydrolyzed at 100 °C for 20 h with 1 mL 30 % HCl (Suprapur®, Merck) per 1 mL of sample and neutralized by acid evaporation under vacuum at 60 °C in a microwave. Samples were analyzed using high-performance liquid chromatography (HPLC) on an Agilent 1260 HPLC system following a modified version of established methods (Lindroth and Mopper, 1979; Dittmar et al., 2009). Prior to the separation of 13 amino acids with a C^{18} column (Phenomenex Kinetex, 2.6 µm, 150 × 4.6 mm), in-line derivatization with *o*-phthaldialdehyde and mercaptoethanol was carried out. A gradient with solvent A containing 5 % acetonitrile (LiChrosolv, Merck, HPLC gradient grade) in a sodium dihydrogen phosphate buffer (Suprapur®, Merck, pH 7.0) and acetonitrile as solvent B was used for analysis. A gradient from 100 % solvent A to 78 % solvent A was produced in 50 min.

2.3 Bacterial production

BP was determined onboard using the ^{3}H–leucine (^{3}H–leu) incorporation technique (Kirchman, 1993) and the microcentrifuge method (Smith and Azam, 1992) for epipelagic water samples. The filtration technique was used for deep-water samples as the centrifuge technique (limited to incubation volumes of 1.5 mL) is not sensitive to deep-water communi-

Table 1. Characteristics of the stations. Lat: latitude; Long: longitude; Bott D: bottom depth; $T_{5\,m}$: temperature at 5 m depth; Ncline depth: nitracline depth, calculated as the layer where NO_3 reaches 50 nM; Pcline depth: phosphacline depth, estimated as the layer where DIP reaches 50 nM; ITchl *a*: 0–250 m integrated total chlorophyll *a*; LIW D: depth of the LIW layer sampled; MDW D: depth of the MDW layer sampled.

	Sampling date (mm/dd/yyyy)	Lat (° N)	Long (° E)	Bott D (m)	$T_{5\,m}$ (°C)	DCM D (m)	Ncline D (m)	Pcline D (m)	ITchl *a* (mg m^{-2})	LIW D (m)	MDW D (m)
ST 10	06/08/2017	37.45	1.57	2770	21.6	89	30	69	28.9	500	1000
FAST	06/03/2017	37.95	2.92	2775	21.0	87	50	59	27.3	350	2500
ST 1	05/12/2017	41.89	6.33	1580	15.7	49	48	76	35.0	500	1000
ST 2	05/13/2017	40.51	6.73	2830	17.0	65	40	70	32.7	500	1000
ST 3	05/14/2017	39.13	7.68	1404	14.3	83	47	100	23.2	450	1000
ST 4	05/15/2017	37.98	7.98	2770	19.0	64	42	63	29.2	500	1000
ST 5	05/16/2017	38.95	11.02	2366	19.5	77	42	78	30.5	200	1000
TYR	05/17/2017	39.34	12.59	3395	19.6	73	82	95	31.3	200	1000
ST 6	05/22/2017	38.81	14.50	2275	20.0	75	43	113	18.7	400	1000
ION	05/25/2017	35.49	19.78	3054	20.6	105	85	231	27.7	250	3000

ties. For SURF and DCM layers, triplicate 1.5 mL samples and a control killed with trichloracetic acid (TCA; 5 % final concentration) were incubated with a mixture of [4,5-^{3}H]-leucine (Amersham, specific activity 112 Ci mmol^{-1}) and nonradioactive leucine at final concentrations of 7 and 13 nM, respectively. Samples were incubated in the dark at the respective in situ temperatures for 1–4 h. On nine occasions during the cruise transect, we checked that the incorporation of leucine was linear with time. Incubations were ended by the addition of TCA to a final concentration of 5 %, followed by three runs of centrifugation at 16 000 g for 10 min. Bovine serum albumin (BSA; Sigma, 100 mg L^{-1} final concentration) was added before the first centrifugation. After discarding the supernatant, 1.5 mL of 5 % TCA was added before the second centrifugation, and after discarding the supernatant, 1.5 mL of 80 % ethanol was added. After the third centrifugation, the ethanol supernatant was then discarded, and 1.5 mL of liquid scintillation cocktail (Packard Ultima Gold MV) was added. For the LIW and MDW layers, 40 mL samples were incubated in the dark for up to 12 h at in situ temperature (triplicate live samples and one control fixed with 2 % formalin) with 10 nM [4,5-^{3}H]-leucine. After filtration of the sample through 0.2 µm polycarbonate filters, 5 % final concentration TCA was added for 10 min; subsequently the filter was rinsed with 10 mL 5 % TCA and a final rinse with 80 % ethanol.

For both types of samples (centrifuge tubes and filters) the incorporated radioactivity was counted using a Packard LS 1600 liquid scintillation counter on board the ship. A factor of 1.5 kg C mol leucine^{-1} was used to convert leucine incorporation to carbon, assuming no isotopic dilution (Kirchman, 1993), as checked four times using concentration kinetics. Standard deviations from triplicate measurements averaged 8 % and 25 % for BP values, estimated with the centrifugation (surface layers) or the filtration technique (deep layers), respectively.

2.4 Ectoenzymatic activities

EEAs were measured fluorometrically using the following fluorogenic model substrates: L-leucine-7-amido-4-methylcoumarin (MCA-leu), 4-methylumbelliferyl–phosphate (MUF–P) and 4-methylumbelliferyl–βD-glucopyranoside (MUF–βglu) to track aminopeptidase (LAP) activity, alkaline phosphatase (AP) activity and β-glucosidase (βGLU) activity, respectively (Hoppe, 1983). Stock solutions (5 mM) were prepared in methyl cellosolve and stored at −20 °C. The numbers of MCA and MUF products released by LAP, AP and βGLU activities after addition of substrate concentrations ranging from 0.025 to 50 µM were followed by measuring the increase in fluorescence (excitation and emission wavelengths 380 and 440 nm for MCA and 365 and 450 nm for MUF, wavelength width 5 nm) in a Varioskan LUX microplate reader. The instrument was calibrated with standards of MCA and MUF solutions diluted in filtered (< 0.2 µm) boiled seawater. For measurements, 2 mL of unfiltered seawater samples was supplemented with 100 µL of a fluorogenic-substrate solution in a black 24-well polystyrene plate in duplicate. Incubations were carried out in the dark in thermostatically controlled incubators at in situ temperatures. Incubations lasted up to 24 h, with fluorescence measurements every 1 to 3 h, depending on the expected activities. The enzyme hydrolysis rate (V) was calculated from the linear part of the fluorescence–time relationship. Boiled-water blanks were run to check for abiotic activity. The parameters Vm (maximum hydrolysis velocity) and Km (Michaelis–Menten half-saturation constant, which reflects enzyme affinity for the substrate) were estimated by fitting the Michaelis–Menten function ($V = \mathrm{Vm} \times S/(\mathrm{Km} + S)$) to the hydrolysis rate (V) as a function of the fluorogenic-substrate concentration (S) using nonlinear regression (PRISM4, Graph Pad software, San Diego, USA). Vm and Km were determined using three

series of substrate concentrations: Vm_{all} and Km_{all} (global model) were calculated using a range of 11 concentrations (0.025, 0.05, 0.1, 0.25, 0.5, 1, 2.5, 5, 10, 25 and 50 µM) in duplicate, Vm_1 and Km_1 (model 1) were calculated using a restricted substrate concentration set (0.025, 0.05, 0.1, 0.25, 0.5 and 1 µM) in duplicate, and Vm_{50} and Km_{50} (model 50) were calculated using the concentration set restricted to the high values of substrate (2.5, 5, 10, 25 and 50 µM). The turnover time was estimated as the ratio Km / Vm (Wright and Hobbie, 1966). We used the term "ectoenzyme" for all types of enzymes found outside the cell, including enzymes attached to external membranes and within the periplasmic space as well as free-dissolved enzymes, to broadly encompass all enzymes located outside of intact cells regardless of the process by which such enzymes interact with the substrate.

We used an approach similar to Hoppe et al. (1993) to compute in situ hydrolysis rates for LAP and βGLU using total carbohydrate (TCHO) and total amino acid (TAA) concentrations in water samples as representative of dissolved carbohydrates and proteins, respectively. The calculation for AP is presented in a companion paper from this issue (Pulido-Villena et al., 2021). These rates were calculated based on both Vm_1 and Km_1 and on Vm_{all} and Km_{all}. In situ hydrolysis rates expressed in nmol substrate $L^{-1}\,h^{-1}$ were converted into carbon and nitrogen units using C / TCHO, C / TAA and N / TAA molar ratios.

2.5 Statistics

To assess biphasic ectoenzymatic activities, all kinetics where the coefficient of variation (standard error/mean ratio) of Vm or Km was greater than 100 % were rejected. For the remaining data we used the F test of Fisher–Snedecor as developed in Tholosan et al. (1999) to ascertain whether two additional parameters (Vm_1, km_1 and $Vm_{50,}$ Km_{50} instead of Vm_{all} and Km_{all}) improved the model significantly based on the following series of equations:

$$\mathrm{Cost(Vm, Km)} = \Sigma\left[\left(V_{\mathrm{data}} - V_{\mathrm{fit}}\right)/w\right]^2, \quad (1)$$

where V_{data} is the experimental hydrolysis rate, V_{fit} is the corresponding value of the fitted function, and w is a weighting factor set to 1, as in Tholosan et al. (1999). The cost function was determined for the global model fitted with the entire set of concentrations ($cost_{all}$), model 1 ($cost_1$) and model 50 ($cost_{50}$) as

$$\mathrm{Var(additional\ parameters)} = \left(\mathrm{cost_{all}} - \mathrm{cost_1} - \mathrm{cost_{50}}\right)/2 \quad (2)$$

$$\mathrm{Var(biphasic)} = \left(\mathrm{cost_1} + \mathrm{cost_{50}}\right)/(n-4), \quad (3)$$

where n is the number of concentration data in the entire data set. These two variances were finally compared using the F test:

$$F_{(2,\,n-4)} = \mathrm{var(additional\ parameters)\,/\,var(biphasic)}. \quad (4)$$

When the F test showed that the variances were significantly different at a probability of 0.1, we assumed that the biphasic mode was meaningful enough to explain the kinetics of the entire data set.

Trends with depth were estimated using a depth variation factor (DVF) estimated as the mean of pooled SURF and DCM data divided by the mean of pooled LIW and MDW data. This decrease (or increase) was considered to be significant after a t test comparing both series of data. The type of t test used depended on the result of a preliminary F test checking for variance. Coefficient of variation (CV) was calculated as standard deviation / mean × 100. Correlations among variables were examined after log transformation of the data. All mean ratios cited in the text were computed from means of ratios and not from the ratio of means.

3 Results

3.1 Physical properties

The physical properties at the sampled stations (Fig. 2) show pronounced longitudinal variation in agreement with the thermohaline circulation features of the Mediterranean Sea (see Introduction). The deep waters, formed by two separate internal-convection cells, have distinct properties in the eastern basin (ION station, temperature of 13.43 °C, salinity of 38.73) and the western basin (the remaining stations, temperature of 12.91 °C, salinity of 38.48). The deep samples of MDW were collected within or in the upper limits of deep waters (Fig. 2). The intermediate-layer samples of LIW were collected in the vicinity of the salinity maxima (Fig. 2), which are used to identify the LIW core (e.g., Wust, 1961). Salinity maxima in the LIW core are particularly pronounced in the west due to the presence of fresher and lighter waters of Atlantic origin above; this feature is progressively relaxed eastward. LIW properties decrease from ION, the closest station from their source, to the westernmost stations of the Algerian Basin (ST10, FAST), concurrent with their westward spread and progressive dilution. During the springtime expedition PEACETIME, the productive layer was stratified with the development of a seasonal thermocline. This interface separated the warm surface waters from the cool waters of Atlantic origin in which the DCM developed. As a consequence, the two sample types collected in the productive layer (SURF and DCM; Fig. 2) have similar salinity but different temperature. For the sake of clarity, the stations are presented according to their longitudinal positions, from west to east in the following order: ST10, FAST, ST1, ST2, ST3, ST4, ST5, TYR, ST6 and ION.

3.2 Biogeochemical properties

Nitrate and phosphate were depleted in the surface layers, with concentrations below the detection limits of classical methods (0.01 µM; Table S1). However, using the LWCC

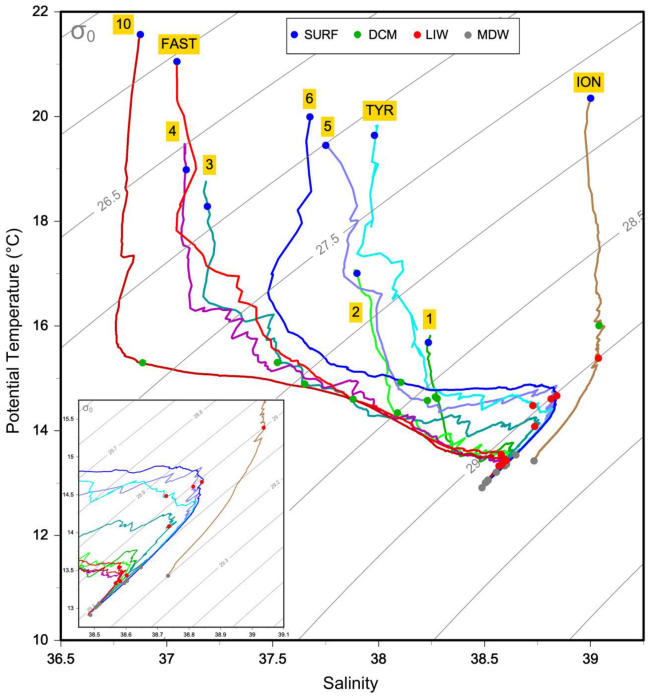

Figure 2. T/S diagram for the sampled stations. Main water masses are as follows. MAW: modified Atlantic water; LIW: Levantine intermediate water; WMDW: western Mediterranean deep water; EMDW: eastern Mediterranean deep water.

technique, which allows the measurement of nanomolar variations in nutrients, DIP could be detected (Table S1) and ranged between 4 and 17 nM at 5 m depth (Table S1). Phosphaclines were deeper than nitraclines and deeper in the eastern basin, particularly at ST 6 and ION. Chlorophyll standing stocks ranged from 18.7 to 35 mg Tchl a m^{-2} at ST 6 and ST1, respectively (integrations down to 250 m; Table 1). The depth of the DCM ranged from 49 to 83 m in the western basin, exhibiting the deepest value in the Ionian Sea (105 m depth at ION), while no obvious trend has been observed in the Tyrrhenian Sea.

DOC ranged from 39 to 75 µM (Table S1). The highest DOC values were generally observed in the surface layers and decreased by approximately 10 µM in each consecutive layer sampled. The DOC depth variation factor ranged from ×1.2 to ×1.6. DON ranged from 2.5 to 10.4 µM. The DON depth variation factor (DVF) was close to that of DOC (×1.2 to ×1.8). DOP ranged from below our detection limit to 0.09 µM. The mean values for the DOC / DON and DOC / DOP molar ratios from all water layers were 14 ± 2 and 2112 ± 1644, respectively, with no significant change in these ratios between epipelagic layers (SURF and DCM) and deeper layers (LIW and MDW) due to the variability between stations. Deep DOP was not sampled at three stations. The DOP estimate is subject to large errors at depth (DIP is on average 10 times higher than DOP).

The mean values of TAAs were similar in the SURF and DCM layers, around 210 nM (Table S1, Fig. S1a), and then decreased in deep layers (LIW and MDW, $p < 0.001$). The mean DVF of TAAs (×3.4) was twice as high as that of DON (×1.5), and as a consequence the TAA-N/DON ratio (Fig. S1a) decreased significantly ($p < 0.001$) in the deep layers compared to the epipelagic layers (Fig. S1a). TCHOs ranged from 111 to 950 nM and the contribution of TCHO-C to DOC from 1.3 % to 9.7 % (Fig. S1b). At 6 stations out of 10, a minimum TCHO value was obtained in the LIW (Fig. S1b). The TCHO-C/TAA-C ratio increased significantly in the deep layers compared to the epipelagic layers ($p < 0.02$) and exhibited particularly high ratios within the Tyrrhenian Sea MDW layer (ST5: 48; TYR: 24; ST6: 27).

3.3 Ectoenzymatic activities – kinetic trends

Examples of different types of kinetics are shown in Fig. 3. In general, the hydrolysis of LAP and βGLU did not completely saturate at 50 µM substrate concentration but started to reach the asymptotic value Vm. The hydrolysis rate of AP reached a maximum around 1 µM MUF–P. In this example, significant fits to Michaelis–Menten kinetics were obtained using all three models. However, significant Michaelis–Menten kinetics were also obtained regardless of the upper limit in the substrate concentration span used for the fit (Fig. S2a, b, c). The Vm and Km characterizing these kinetics increased with the highest concentration included in the set, reaching a plateau towards the set with the largest span (more rapidly for AP; Fig. S2c and f). In order to check for the presence of biphasic kinetics and the effect of choosing two extreme sets of concentrations ranges, to determine EEA kinetic parameters we systematically used the three models described in Sect. 2.4. The set of model 1 in the lower range of substrate concentration represents a compromise between having a sufficient set of substrate concentrations and significant enzymatic rates detected. Some kinetics were discarded (i) due to the detection limits at a low concentration of substrates (it was the case for all the βGLU estimates in LIW and MDW layers; Table S2) or (ii) due to a significant deviation from the model (in particular, when the rates did not increase between 2.5 and 50 µM substrate concentration, leading to abnormally low values of Km_{50}). This occurred in particular for AP, with only 25 kinetics out of 40 showing significant Michaelis–Menten kinetic estimates of the model based on high concentrations of substrates (see AP model 50; Table S2).

For LAP and βGLU, Vm_{all} and Vm_{50} were close; the distribution of these data fit the 1 : 1 axis (Fig. 4). For LAP and AP, Vm_{50} was subjected to higher errors than those of their corresponding Vm_{all} (Fig. 4) as the percentage of standard error (SE %; Table S2) of Vm_{50} was higher than that of Vm_1 in most cases (40/40 for LAP, 24/25 for AP). In contrast, for βGLU SE % was higher only in 6 out of 20

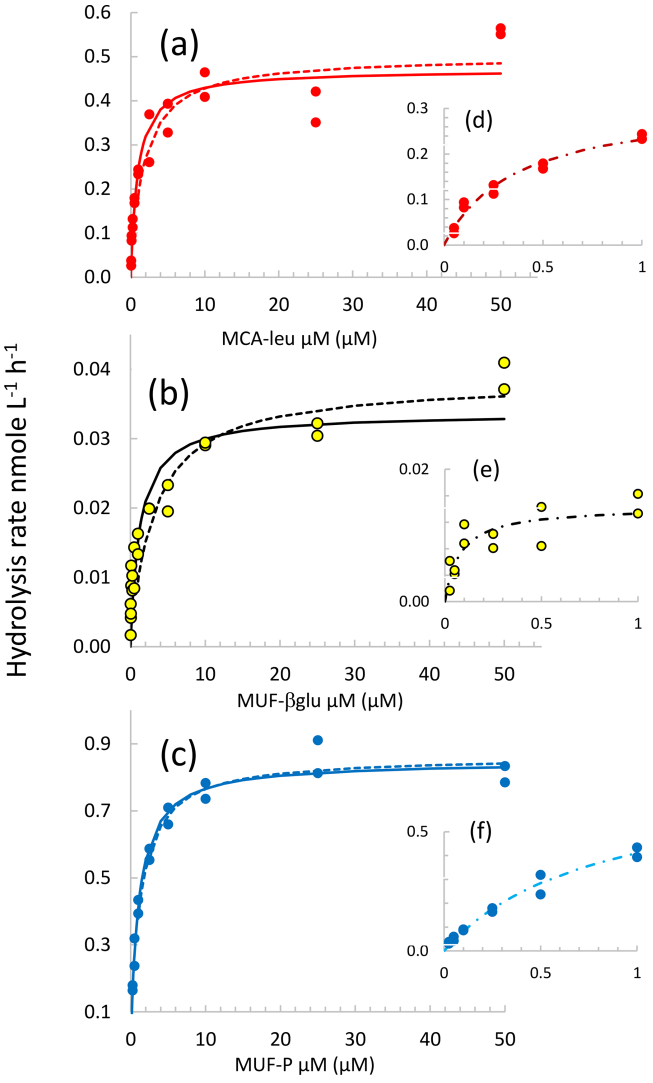

Figure 3. Michaelis–Menten kinetics for the DCM layer at station FAST. **(a, b, c)** Data are shown by the dots, continuous lines correspond to the nonlinear regression of the global model (concentration set 0.025 to 50 µM), and dotted lines correspond to the nonlinear regression of model 50. **(d, e, f)** Michaelis–Menten kinetics for model 1 (concentration set 0.025–1 µM).

cases. The relationships between Km_{50} and Km_{all} showed the same trend, although Km_{50} was generally slightly higher than their corresponding Km_{all}, in particular for βGLU. As noted for Vm, the SE % was higher for Km_{50} than for Km_1 in most of the cases for LAP (39/40) and AP (25/25), and the opposite was seen for βGLU (5/20). The standard errors in Km were higher than those in their corresponding Vm (Table S2). For LAP and βGLU, Vm_1 was notably lower than Vm_{50} and Vm_{all}, and Km_1 was notably lower than Km_{50} and Km_{all}. For AP, the difference between Vm_1 and Vm_{50} was not so evident, Vm_1 being closer to Vm_{50}. However, Km_{50} was generally still much higher than Km_1.

The biphasic mode itself explained the kinetics of the entire data set in 17 cases out of 40 for LAP, in 18 cases out of 20 for βGLU and in 18 cases out of 24 for AP (Table S2). Thus, the biphasic mode was enough on average to explain 60 % of the cases, with the highest proportions for βGLU. We estimated the degree of difference between the two kinetics using the "biphasic indicator" developed in Tholosan et al. (1999). This index tracks the difference between the initial slopes (Vm / Km) of Michaelis–Menten kinetics as $(Vm_1 / Km_1) / (Vm_{50} / Km_{50})$. The biphasic indicator was particularly marked for βGLU (means of 87 in SURF and 47 in DCM layers), but it was highly variable (Table S2). For LAP the mean index increased from ∼9 in SURF and DCM layers to ∼16 within LIW and MDW layers; however, due to the variability in the indicator (Table S2), this increase was insignificant. For AP the biphasic indicator remained constant ($p>0.05$) between epipelagic layers (means of 12 in SURF and 6 in the DCM) and deeper layers sampled (mean of 5 in LIW and 9 in the MDW, respectively, with overall lower variability than for the two other enzymes; Table S2).

As the constants Km and Vm provided by the global model were very close to those of model 50, as the standard errors were mostly higher for model 50, and as the biphasic mode was not observed in all samples, we present here the kinetic parameters for the global model and model 1 (Figs. 5, 6 and 7 and Table 2). Moreover, the lowest-concentration range is closer to natural substrate concentrations.

For each enzyme (LAP, βGLU, AP) and the two models (model 1, global model), Vm was of the same order of magnitude at the SURF and DCM layers (Figs. 5, 6, 7). In all layers, the highest mean Vm was obtained for AP, followed by LAP and then βGLU, independently of the model used (Table 2).

For LAP (Fig. 5), Vm_{all} was on average 3 times higher than Vm_1 in both SURF and DCM layers, but the differences between these two rates increased with depth (×8 in LIW layers, ×12 in MDW layers). Vm_{all} decreased from epipelagic to mesopelagic layers by a factor of ×8 on average, while Vm_1 decreased by a factor ×19 (Fig. 5a). However, the decrease was more prominent at stations ST10 to ST5 in the western basin, while in Tyrrhenian waters (ST5, TYR and ST6) Vm_{all} did not show such a marked decrease with depth. The average Km_{all} / Km_1 ratio for LAP was 132. Km_{all} of LAP showed variable patterns with depth. Within the LIW and MDW layers, Km_{all} was of the same order of magnitude as in the surface, sometimes even higher (FAST, ST 3, ST5, ST6, ION), particularly in the Tyrrhenian and Ionian seas (Fig. 5b). Km_1 decreased with depth at the western stations (ST10 to ST3), whereas for stations 4, 6 and ION Km_1 was of the same order of magnitude at all depths.

For the LIW and MDW layers, βGLU kinetics could not be assessed since an increase in fluorescence versus time was found only for the higher substrate concentrations used. The means of βGLU rates measurable at depth

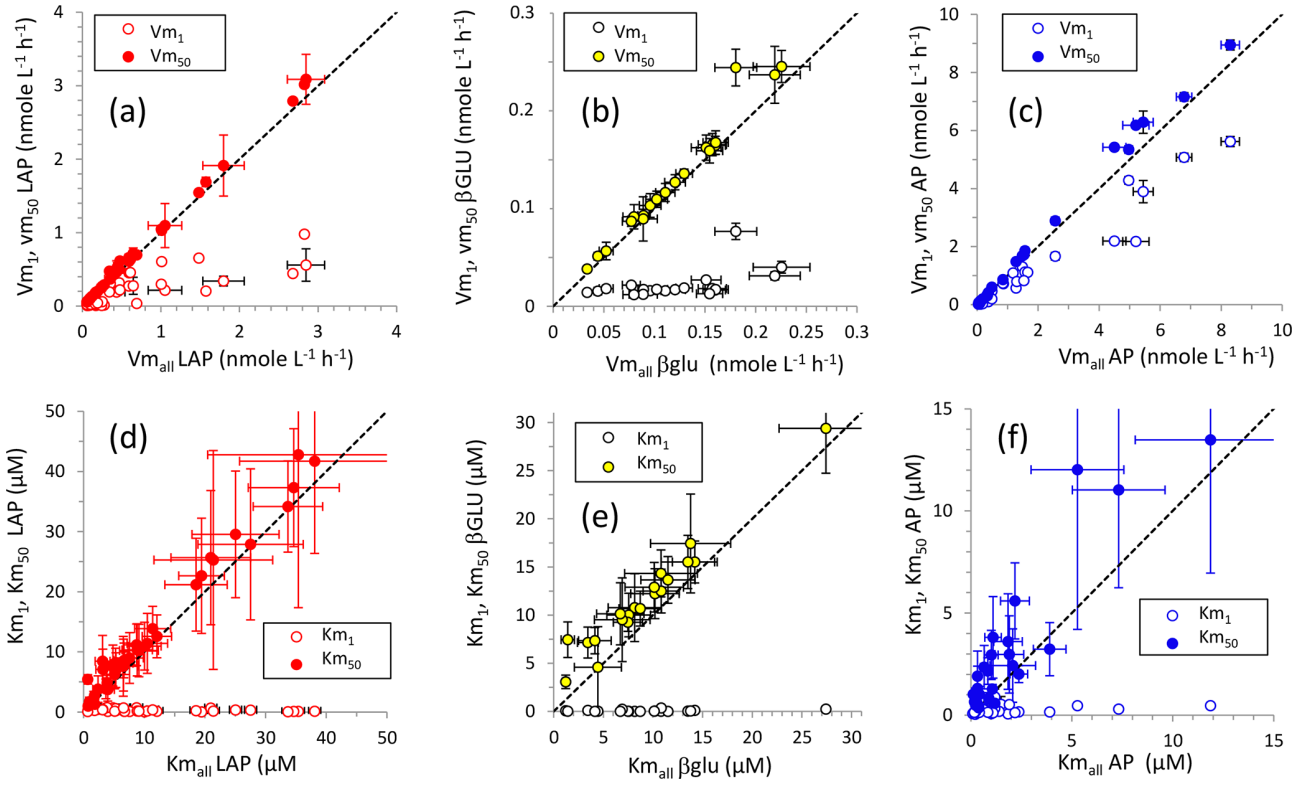

Figure 4. Relationships between kinetic parameters resulting from model 1, model 50 and the global model for the three ectoenzymes: **(a, d)** leucine aminopeptidase (LAP), **(b, d)** β-glucosidase (βGLU) and **(c, f)** alkaline phosphatase (AP). **(a, c, f)** Relationships between Vm_1 and Vm_{all} and between Vm_{50} and Vm_{all}; **(d, e, f)** relationships between Km_1 and Km_{all} and between Km_{50} and Km_{all}. Error bars show standard errors. The standard error in Km_{all} in **(d)**, **(e)** and **(f)** (white dots) is not plotted for clarity.

were 0.010 ± 0.006 nmol L^{-1} h^{-1} in the LIW layer and 0.008 ± 0.006 nmol L^{-1} h^{-1} in the MDW layer (Fig. 6, Table 2). In the epipelagic layers (Fig. 6), Vm_{all} was on average 7 and 5 times higher than Vm_1 in SURF and DCM layers, respectively. The ratio Vm_{all}/Vm_1 was greater than those observed in the same layers for LAP or AP (Fig. 6a). The average Km_{all}/Km_1 ratio for βGLU was 311. While Km_{all} was of the same order of magnitude or slightly lower in the DCM compared to the SURF layers, the opposite trend was observed for Km_1, which tended to be higher within the DCM layer (Fig. 6b). Among the three ectoenzymes, βGLU showed the lowest longitudinal variability within surface layers (the longitudinal coefficient of variation (CV) was 34 % for Vm_{all} and 45 % for Vm_1).

AP was the enzyme for which Vm_1 and Vm_{all} were the closest (the average Vm_{all}/Vm_1 ratio for the whole data set was 1.9 ± 1.2) (Figs. 4c, 7a). Fits to model 50, using 2.5 to 50 µM concentration sets, were often not significant (Table S2) because the rates stayed constant when adding these concentrations. AP within the SURF layer showed pronounced relative longitudinal variability, with longitudinal CV close to 100 % for Vm_{all} and Vm_1 (Table 2). Within the SURF layers AP increased towards the east, from a range of 0.5–0.9 nmol L^{-1} h^{-1} for Vm_{all} at ST10 and FAST up to 8 nmol L^{-1} h^{-1} at ION. Both AP Vm_1 and Vm_{all} decreased with depth (Fig. 7a), although both AP Vm_{all} and AP Vm_1 could be higher within the DCM layer than in the SURF layer (ST1, 2, 5 TYR, ION). At all stations Vm in the MDW was equal to or lower than that in the LIW. DVF was large, varying from ×1.8 to ×71 for Vm_{all}, with lower values at ST10 (×1.8), FAST (×3.2) and ST3 (×2.4) and the highest DVF at ST1 (×34), ST2 (×71) and ION (×54). AP Km_{all} was on average 6 times higher than Km_1. Km_{all} increased more with depth (DVF > 0 at eight stations and ranging from ×1.4 to ×19) than Km_1 (DVF > 0 at nine stations and ranging ×1.9 to ×3.8; see ST1 and ST5). However, these differences between AP Km_1 and AP Km_{all} were still the lowest compared to the two other enzymes.

The turnover time of ectoenzymes (Km / Vm ratio) drives the activity at low concentrations of substrates. The incidence of the tested set of substrate concentration is very important in this parameter as turnover times are systematically lower for the 0.025–1 µM concentration set (Table 3). The turnover times were the shortest for AP and the longest for βGLU.

Table 2. Heterotrophic bacterial abundances (BAs), bacterial production (BP) and ectoenzyme kinetic parameters of the global model (Vm_{all}, Km_{all}) obtained from the entire substrate range (0.025 to 50 µM) and of model 1 (Vm_1, Km_1) obtained from the low substrate range (0.025 to 1 µM) for leucine aminopeptidase (LAP), β-glucosidase (βGLU) and alkaline phosphatase (AP) at the four layers. Mean ± SD and range values given for all stations. Maximum velocity rates (Vm_{all} and Vm_1), half-saturation constants (Km_{all} and Km_1); nk: no kinetics available as there are not enough significant rates to plot Michaelis–Menten kinetics.

		SURF	DCM	LIW	MDW
Vm_{all} LAP	Mean ± SD	0.97 ± 0.79	1.20 ± 0.92	0.22 ± 0.18	0.15 ± 0.08
nmol L^{-1} h^{-1}	Range	0.36–2.85	0.35–2.83	0.08–0.69	0.06–0.28
Vm_1 LAP	Mean ± SD	0.29 ± 0.10	0.45 ± 0.25	0.028 ± 0.014	0.017 ± 0.010
nmol L^{-1} h^{-1}	Range	0.21–0.56	0.19–0.98	0.014–0.060	0.007–0.042
Vm_{all} βGLU	Mean ± SD	0.13 ± 0.04	0.11 ± 0.06	nk	nk
nmol L^{-1} h^{-1}	Range	0.08–0.23	0.03–0.22		
Vm_1 βGLU	Mean ± SD	0.019 ± 0.009	0.025 ± 0.019	nk	nk
nmol L^{-1} h^{-1}	Range	0.012–0.040	0.014–0.077		
Vm_{all} AP	Mean ± SD	2.52 ± 2.62	3.73 ± 4.52	0.38 ± 0.48	0.24 ± 0.40
nmol L^{-1} h^{-1}	Range	0.30–8.30	0.11– 14.6	0.04–1.66	0.06–1.30
Vm_1 AP	Mean ± SD	1.55 ± 1.58	3.01 ± 4.01	0.24 ± 0.33	0.12 ± 0.25
nmol L^{-1} h^{-1}	Range	0.25–5.62	0.07–13.2	0.02–1.11	0.01–0.80
Km_{all} LAP	Mean ± SD	6.0 ± 5.6	5.3 ± 7.6	16.4 ± 13.3	15.2 ± 11.3
µM	Range	0.8–20.9	0.7–25.0	3.6–38.1	1.8–34.6
Km_1 LAP	Mean ± SD	0.49 ± 0.18	0.43 ± 0.27	0.23 ± 0.19	0.13 ± 0.11
µM	Range	0.12–0.70	0.07–0.90	0.10–0.69	0.01–0.39
Km_{all} βGLU	Mean ± SD	10.6 ± 6.3	7.7 ± 5.1	nk	nk
µM	Range	4.4–27.4	1.2–14.2		
Km_1 βGLU	Mean ± SD	0.044 ± 0.071	0.11 ± 0.11	nk	nk
µM	Range	0.009–0.244	0.01–0.36		
Km_{all} AP	Mean ± SD	0.58 ± 0.67	0.49 ± 0.34	2.25 ± 2.42	2.6 ± 3.5
µM	Range	0.09–2.18	0.18–1.07	0.17–7.32	0.4–11.9
Km_1 AP	Mean ± SD	0.11 ± 0.03	0.27 ± 0.28	0.37 ± 0.22	0.27 ± 0.16
µM	Range	0.07–0.14	0.05–0.80	0.14–0.89	0.06–0.52
BAs	Mean ± SD	5.3 ± 1.6	5.4 ± 1.5	1.13 ± 0.40	0.56 ± 0.15
10^5 cells mL^{-1}	Range	2.1–7.8	4.0–8.5	0.41–1.91	0.33–0.78
BP	Mean ± SD	37 ± 13	21 ± 7	0.77 ± 0.40	0.27 ± 0.19
ng C L^{-1} h^{-1}	Range	26–64	12–32	0.39–1.60	0.07–0.60

3.4 Specific activities

BP was of the same order of magnitude within SURF and DCM layers (Fig. S3, Table 2) and decreased towards deeper layers (DVF 59 ± 23). BA varied less than ectoenzyme Vm or BP longitudinally. Further, the decrease in BA with depth was less pronounced (DVF 7 ± 2) than BP. Cell-specific BP (cs-BP) ranged from 1 to 136×10^{-18} g C $cell^{-1}$ h^{-1} (Table 4), decreasing with depth at all stations (DVF ranged from ×4 to ×23). For enzymes and BP (Figs. 8 and 9, Table 2), the trend of specific activities was highly variable, with the highest DVF (decrease with depth) observed for cs-BP or cs-AP.

For LAP, specific activities ranged from 0.1–2.1 $\times 10^{-18}$ to 0.7–8 $\times 10^{-18}$ mol leu $cell^{-1}$ h^{-1}, based on Vm_1 and Vm_{all} rates, respectively (Fig. 8a, b; Table 4 for Vm_1). A significant decrease with depth from epipelagic waters to deep waters was only found for cs-Vm_1 LAP but not for cs-Vm_{all} LAP ($p < 0.001$; Fig. 9a). While cell-specific LAP Vm_1 decreased with depth, the LAP Vm_1 per unit BP increased with depth at all stations (Table 4, Fig. 9a).

For AP, specific activities ranged from 0.11 to 32×10^{-18} mol P $cell^{-1}$ h^{-1} and from 0.14 to 39×10^{-18} mol P $cell^{-1}$ h^{-1} based on Vm_1 and Vm_{all} rates, respectively, not differing significantly due to the small

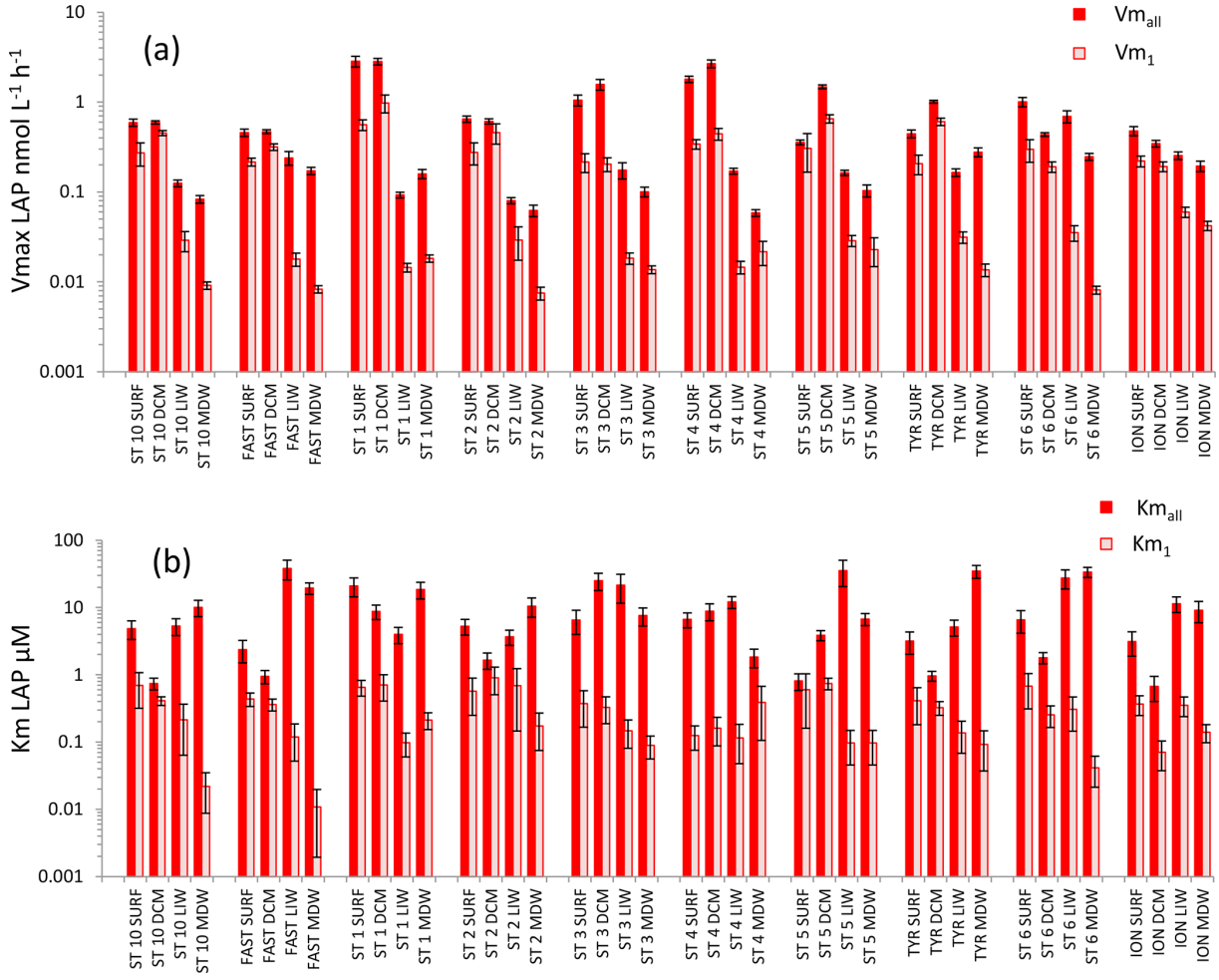

Figure 5. Distribution of kinetic parameters Vm **(a)** and Km **(b)** for leucine aminopeptidase (LAP) calculated from model 1 (Vm_1, Km_1) and the global model (Vm_{all}, Km_{all}). Error bars represent the standard errors derived from the nonlinear regressions.

Table 3. Turnover times of ectoenzymes (Km / Vm ratio). Mean ± SD and range values given. For leucine aminopeptidase (LAP), β-glucosidase (βGLU) and alkaline phosphatase (AP). The turnover times are calculated from the global model (Km_{all} / Vm_{all}) or the model 1 (Km_1 / Vm_1); nk: no kinetics available as there are not enough significant rates to plot Michaelis–Menten kinetics.

	Units: days	SURF	DCM	LIW	MDW
Km_{all} / Vm_{all} LAP	Mean ± SD	255 ± 79	158 ± 182	3394 ± 2629	4161 ± 1806
	Range	94–340	40–663	1294–9016	1308–7028
Km_1 / Vm_1 LAP	Mean ± SD	74 ± 26	42 ± 22	345 ± 235	343 ± 298
	Range	15–106	15–82	141–985	55–959
Km_{all} / Vm_{all} βGLU	Mean ± SD	3464 ± 1576	3091 ± 1551	nk	nk
	Range	1997-7395	328-5481		
Km_1/Vm_1 βGLU	Mean ± SD	126 ± 233	247 ± 273	nk	nk
	Range	20-784	15-873		
Km_{all} / Vm_{all} AP	Mean ± SD	12 ± 9	39 ± 46	563 ± 542	914 ± 817
	Range	2–33	0.7–113	16–1441	20–2719
Km_1/Vm_1 AP	Mean ± SD	5.6 ± 5.0	27 ± 37	268 ± 349	301 ± 172
	Range	1–17	0.6–106	12–1180	14–594

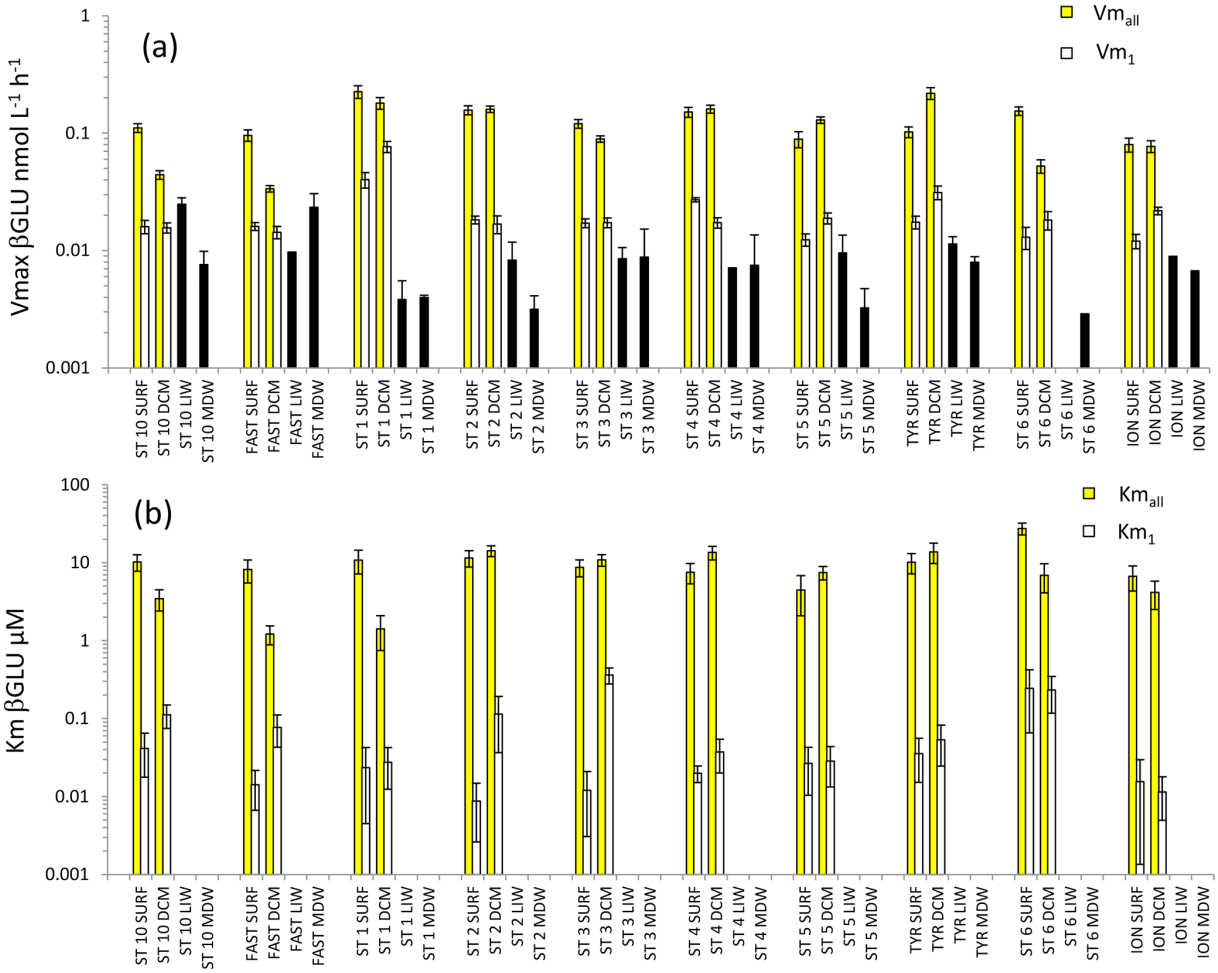

Figure 6. Distribution of kinetic parameters Vm **(a)** and Km **(b)** for β-glucosidase (βGLU) calculated from model 1 (Vm_1, Km_1) and the global model (Vm_{all}, Km_{all}) in SURF and DCM. Error bars represent the standard errors derived from the nonlinear regressions. In the LIW and MDW layers, kinetics were impossible to compute due to the low number of measurable rates (see results). The black bar in **(a)** is assumed to represent a minimal value for Vm_{all}.

differences between AP Vm_1 and AP Vm_{all} (Fig. 8c, d). Cs-AP exhibited either an increase (DVF < 1) or a decrease (DVF > 1) with depth (Fig. 9b). AP Vm_1 per unit BP decreased with depth at all stations except at ION, whereas AP Vm_1 per unit cell increased in 7 cases out of 10.

3.5 In situ hydrolysis rates

The in situ hydrolysis rates of TAAs by LAP were higher: ~ 3 times higher in epipelagic and ~ 7 times higher in deep waters with the model 1 constants as compared to the global model (Fig. 10). Km_{all} was much higher than TAA concentrations (26- to 300-fold depending on the layers; Tables 2, S1). This difference was also the case for Km_1, but the ratio between Km_1 and TAAs differed by factors of 2 to 3 depending on depth layer. Consequently, in situ TAA hydrolysis rates by LAP based on the global model represented a small percentage of Vm_{all} (highest means of 11 % in the DCM and minimum mean value 0.6 % in the MDW). However, in situ rates based on model 1 represented a higher proportion of Vm_1 (means of 30 % to 39 % depending on the layer).

The in situ hydrolysis rates of TCHOs by βGLU were ~ 2.5 times higher using model 1 than using global model in epipelagic layers (Fig. 11). Km_{all} was higher than in situ TCHO concentrations (Tables 2, S1) by a factor of ~ 18 within SURF and 22 within the DCM. Consequently, in situ βGLU hydrolysis rates based on the global model were quasi-proportional to the turnover rate Vm_1 / Km_1 and represented a mean of 7 % of the Vm_{all} in epipelagic layers. Km_1 was much lower than in situ TCHO concentrations (by a factor of ~ 31 in SURF and 8 at the DCM), and thus most in situ rates based on model 1 were close to Vm_1 (93 % in SURF, 79 % at the DCM).

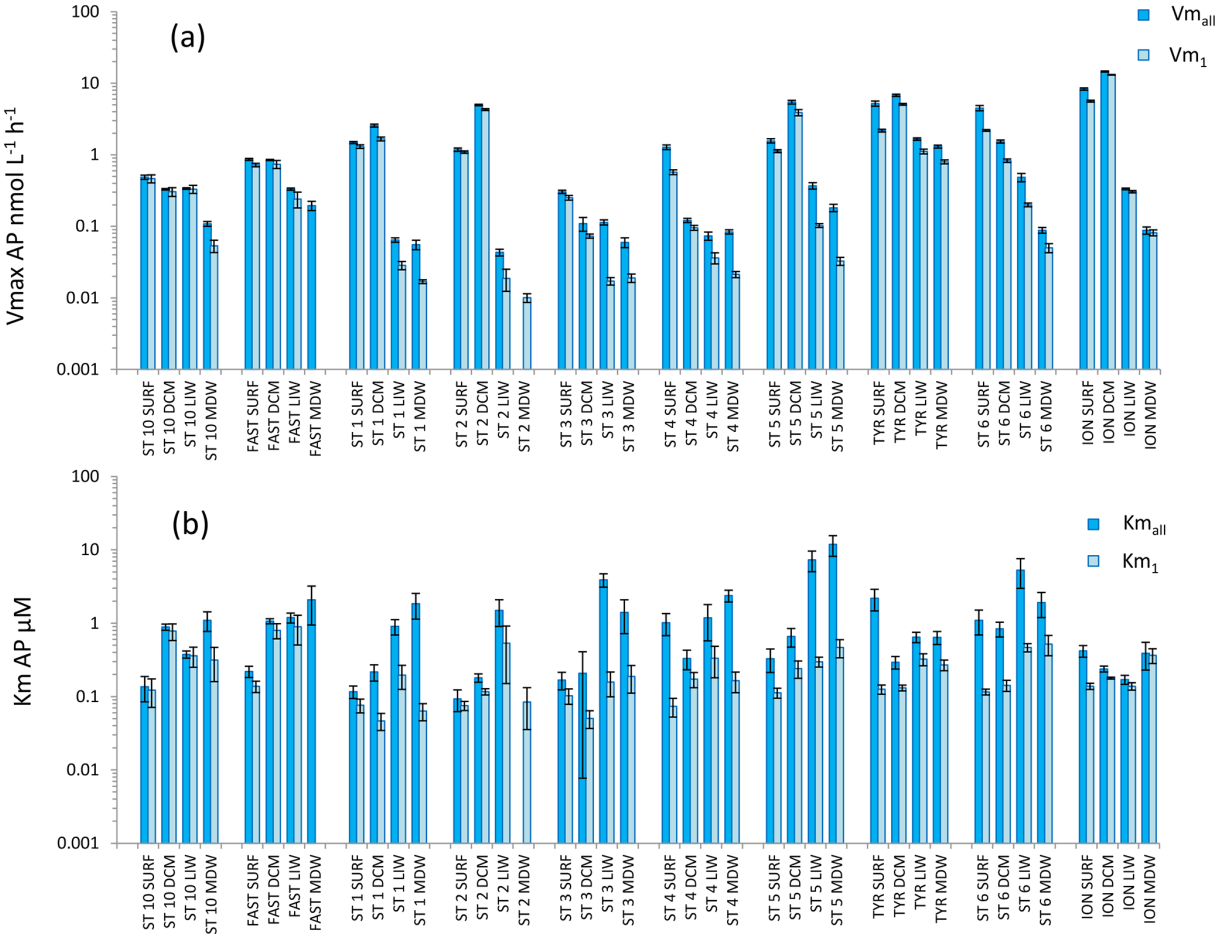

Figure 7. Distribution of kinetic parameters Vm **(a)** and Km **(b)** for alkaline phosphatase (AP) calculated from model 1 (Vm_1, Km_1) and the global model (Vm_{all}, Km_{all}). Error bars are the standard errors derived from the nonlinear regressions.

Table 4. Range of different specific activities calculated using Vm_1 and specific to either (i) abundance of total heterotrophic prokaryotes (cell-specific – cs – activities) or (ii) heterotrophic bacterial production (per BP LAP, per BP βGLU, per BP AP). DVF is the "depth variation factor", calculated for each station as the mean value in epipelagic water (SURF and DCM data) divided by the mean in deep waters (LIW and MDW). The distribution of cs-Vm_1 and cs-Vm_{all} for AP and LAP is also presented in Fig. 8. nd: not determined.

Enzyme	Units	SURF	DCM	LIW	MDW	DVF
cs-LAP	10^{-18} mol leu cell^{-1} h^{-1}	0.33–1.52	0.44–2.18	0.11–0.70	0.13–0.54	1.3–9.6
cs-βGLU	10^{-18} mol glucose cell^{-1} h^{-1}	0.02–0.11	0.02–0.17	nd	nd	nd
cs-AP	10^{-18} mol P cell^{-1} h^{-1}	0.45–26	0.11–32	0.13–11	0.17–23	0.1–28
cs-BP	10^{-18} g C cell^{-1} h^{-1}	46–136	25–60	3–17	1–14	4–23
Per BP LAP	nmol AA nmol C^{-1}	0.04–0.24	0.12–0.44	0.21–1.08	0.36–3.03	0.09–0.76
Per BP βGLU	nmol glucose nmol C^{-1}	0.003–0.017	0.007–0.034	nd	nd	nd
Per BP AP	nmol P nmol C^{-1}	0.09–2.3	0.05–11	0.46–8	0.6–40	0.04–1.7

4 Discussion

4.1 The use of a broader set of substrate concentrations changes our interpretation of ectoenzyme kinetics

The idea that ectoenzyme kinetics are not monophasic is neither new nor surprising (Sinsabaugh and Follstad Shah, 2012,

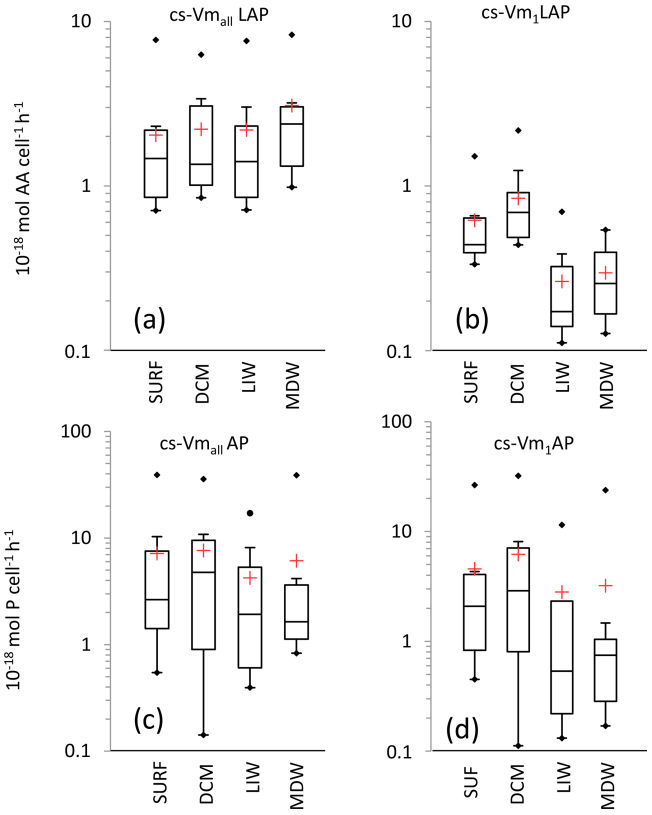

Figure 8. Box plot distributions of cell-specific (cs) Vm_1 and Vm_{all} for leucine aminopeptidase **(a, b)** and alkaline phosphatase **(c, d)**. Box limits are the 25 % and 75 % percentiles; the horizontal bar is the median; the red cross is the mean; black dots are outliers.

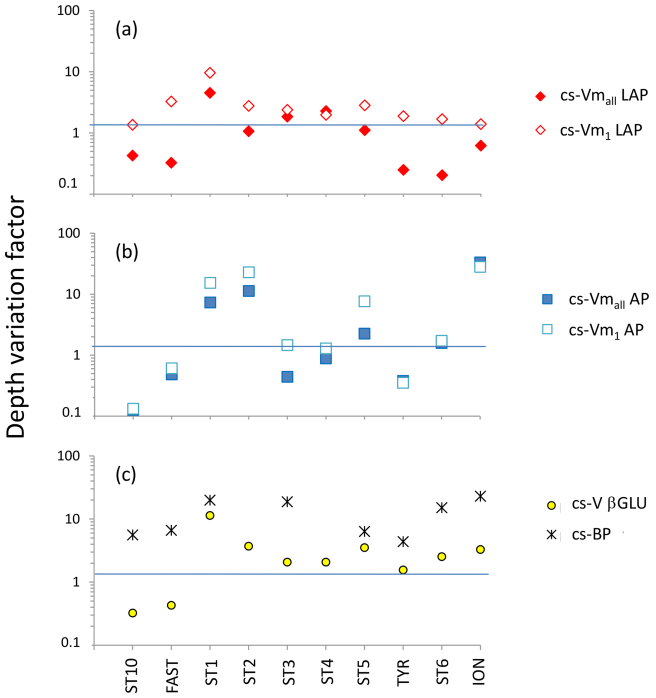

Figure 9. Depth variation factor (DVF; unitless) for ectoenzymatic specific activities. DVF is calculated as the mean of pooled data from the SURF and DCM layers divided by the mean of pooled data from the LIW and MDW layers. **(a)** DVF of cell-specific leucine aminopeptidase (cs-Vm_{all} and cs-Vm_1); **(b)** DVF of cell-specific alkaline phosphatase (cs-Vm_{all} and cs-Vm_1); **(c)** for β-glucosidase DVF, cell-specific activities are based on the few detectable rates at high concentration (yellow dots). Black crosses show the DVF of cell-specific heterotrophic prokaryotic production (cs-BP).

and references therein). However, despite the "sea of gradients" encountered by marine bacteria (Stocker, 2012), multiphasic kinetics are seldom considered. In this work, we attempt to compare different concentration sets of fluorogenic substrates in order to evaluate the consequences for the estimated kinetic parameters in relation to the in situ natural concentrations of the substrates. In the coastal, epipelagic waters of the Mediterranean Sea, Unanue et al. (1999) used a set of concentrations ranging from 1 nM to 500 µM to reveal biphasic kinetics with a switch between the two phases at around 10 µM for LAP and 1–25 µM for βGLU. They referred to "low-affinity" enzymes and "high-affinity" enzymes. In the Toulon Bay (NW Mediterranean Sea), Bogé et al. (2012) used a MUF–P range from 0.03 to 30 µM and described biphasic AP kinetics, with a switch between the two enzymatic systems around 0.4 µM. In our study, the biphasic indicator $(Km_{50} / Vm_{50})/(Km_1 / Vm_1)$ was used to determine the degree of difference between the two Michaelis–Menten LAP kinetics. The differences between the two LAP enzymatic systems in the water column increased with depth and could be as large as that found in sediment (biphasic indicator of 20; Tholosan et al., 1999), in which large gradients of organic matter concentrations are found. However, this was not the case for all enzymes: for AP, the differences were small and consistent with depth gradients. The differences between the high- and low-affinity enzyme were greater for βGLU.

By comparing model 1, model 50 and the global model and from the analysis presented in Fig. S2, it is clear that the choice of the highest concentration used in the Michaelis–Menten kinetics is crucial. We thus decided not to focus our discussion on the presence of biphasic kinetics or lack thereof. Rather, we compared the effects of choosing a set of concentration ranges sufficiently low to obtain measurable rates but at the same time encompassing the natural range of substrates (model 1 representing the high-affinity system). We discuss the enzymatic properties obtained with the global model, which refers better to the concentration generally used in the literature but also reflected a low-affinity system compared to model 1.

Enzymatic kinetic parameters are also relevant for the interpretation of the hydrolysis of the substrate in terms of quality and quantity. For instance, the LAP Km_{all} is much higher than βGLU Km_{all} probably because LAP is not selected for low-concentration ranges, in contrast to βGLU (Christian and Karl, 1995) and AP. It is also possible, how-

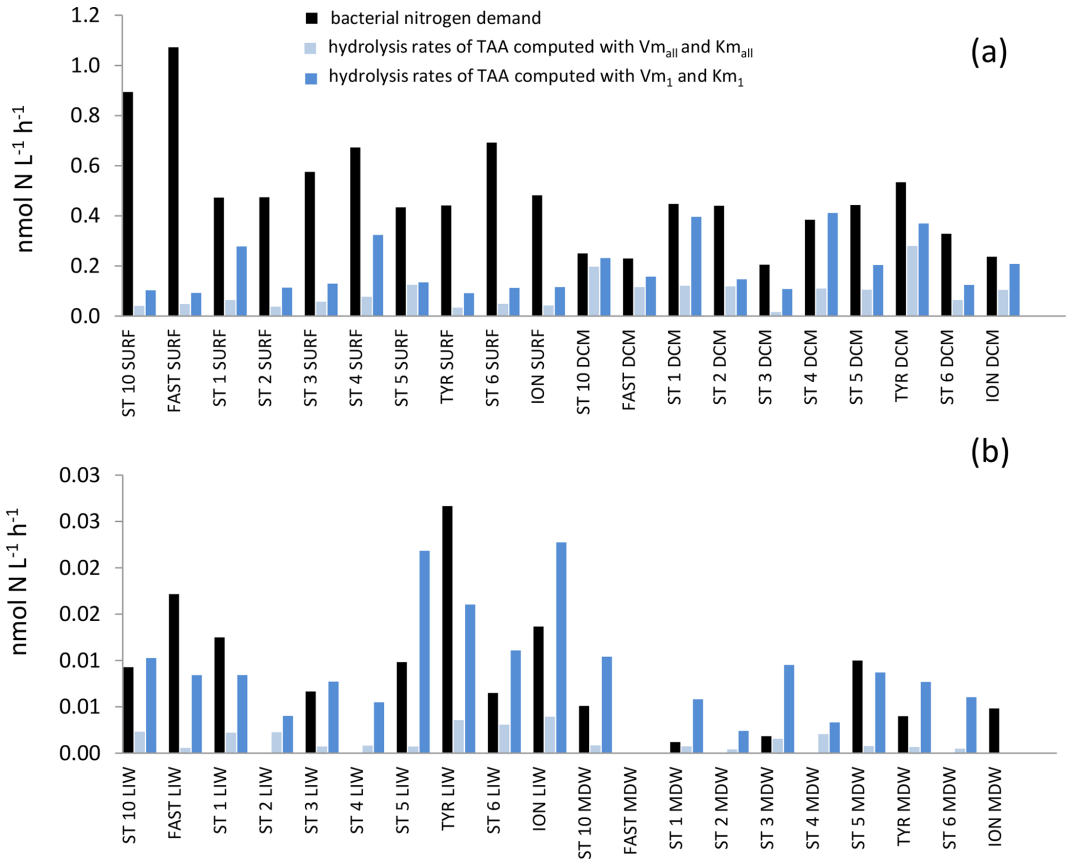

Figure 10. In situ hydrolysis rates of proteins (nmol N L^{-1} h^{-1}), determined from TAA and LAP ectoenzyme kinetics for the high- and low-affinity systems, and heterotrophic bacterial nitrogen demand, determined from BP assuming a C/N molar ratio of 5 and no active excretion of nitrogen. **(a)** Epipelagic layers (SURF, DCM), **(b)** deeper layers (LIW, MDW).

ever, that when the fluorogenic substrates are in the same concentration range as the natural substrates, this leads to a competition for the active sites. We can surmise that Km_1 values, although lower than published values, are still potentially overestimated. Another difference in the response to the tested range of concentrations for each substrate is the Km / Vm ratio: a lower ratio indicates the adaptation to hydrolyze substrates at low concentrations. This should be considered carefully when comparing reported values.

We have shown that the differences between the Km and Vm of the low- and high-affinity enzymes might change with the nature of the enzyme, with depth and regionally. We will develop the different interpretation emerging from (i) the increase or decrease with depth, (ii) the use of enzymatic ratio as indicators of nutrient availability or DOM quality, and (iii) the estimates of in situ hydrolysis rates and their contribution to heterotrophic bacterial carbon or nitrogen demand.

4.2 How the set of concentrations used affects ectoenzymatic kinetic trends with depth: possible links with access to particles

As shown by this study, depending on the range of concentrations tested, different conclusions can be drawn regarding the increase or at least maintenance of specific levels of activity within deep layers (Koike and Nagata, 1997; Hoppe and Ulrich, 1999; Baltar et al., 2009b). Many factors, such as the freshness of the suspended particles, particle fluxes, a recent convection event, lateral advection, and the seasonality and taxonomic composition of phytoplankton, could influence dynamics at depth, particularly in the mesopelagic layers (Tamburini et al., 2002, 2009; Azzaro et al., 2012; Caruso et al., 2013; Severin et al., 2016).

AP was the enzyme that showed the smallest contrasts between different kinetics. In this study, the use of MUF–P concentrations ranging between 0.025 and 50 µM highlighted that AP rates are well described with the Michaelis–Menten kinetic model 1, with saturation reached around 1 µM. We thus assumed that this AP activity should belong to free-living bacteria and/or dissolved enzymes (< 0.2 µm fraction)

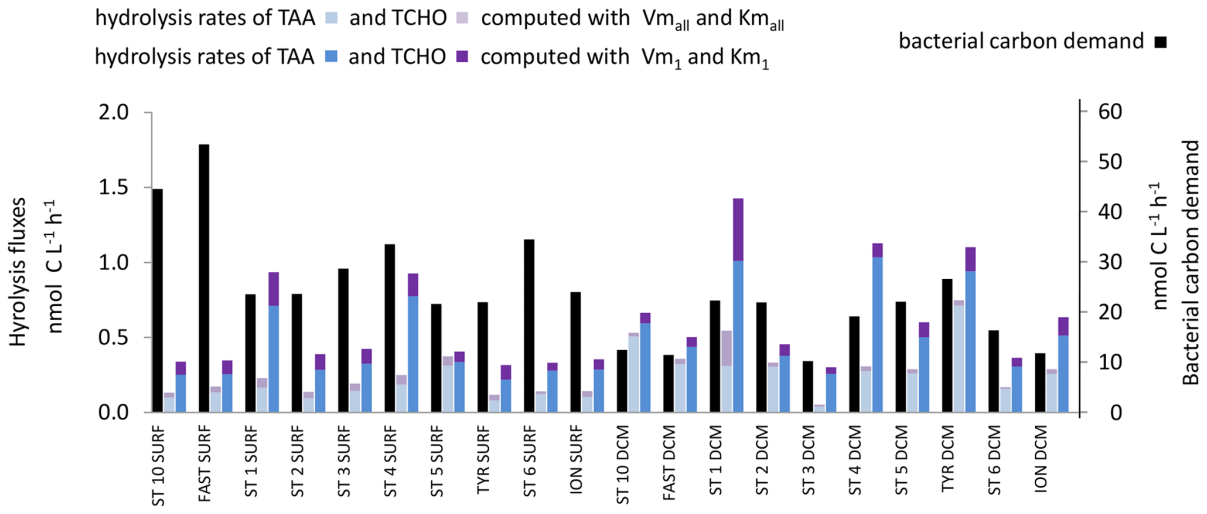

Figure 11. In situ hydrolysis rates of carbohydrates and proteins (nmol C L^{-1} h^{-1}), determined from TAAs, TCHOs, and LAP and βGLU ectoenzymatic kinetics for the low- and high-affinity systems, and heterotrophic bacterial carbon demand (BCD), determined from BP assuming a bacterial growth efficiency of 10 % in epipelagic waters. Note the different scale for bacterial carbon demand on the right.

adapted to low substrate concentrations. These results agree with the DOP concentrations measured, ranging between 12 and 122 nM in epipelagic waters (Pulido-Villena et al., 2021) and, when detectable, between 20 and 51 nM in deep layers. Using fractionation–filtration procedures, it has been shown that more than 50 % of the AP activity could be measured in the < 0.2 µm size fraction (Baltar, 2018, and references therein), whereas the dissolved fraction of other enzymes is generally lower. Hoppe and Ulrich (1999) found a contribution by the < 0.2 µm fraction of 41 % for AP, 22 % for LAP and only 10 % for βGLU. During the PEACETIME cruise we ran a few size fractionation experiments in SURF and DCM samples (results not shown). The contribution of the < 0.2 µm fraction to the bulk activity was on average 60 ± 34 % ($n = 12$) for AP, 25 ± 16 % ($n = 12$) for βGLU and 41 ± 16 % ($n = 12$) for LAP, confirming these trends in the Mediterranean Sea.

Increasing AP activities per cell with depth have been reported in the Indian Ocean (down to 3000 m depth; Hoppe and Ullrich, 1999), in the subtropical Atlantic Ocean (down to 4500 m depth; Baltar et al., 2009b) and in the central Pacific Ocean (down to 4000 m depth; Koike and Nagata, 1997). These authors used high concentrations of MUF–P (150 to 1200 µM) that could stimulate ectoenzymes of cells attached to suspended or sinking particles and thus adapted to higher-concentration ranges. However, these trends were also obtained using low concentrations (max 5 µM MUF–P), at depths down to 3500 m in the Tyrrhenian Sea (Tamburini et al., 2009). In the bathypelagic layers of the central Pacific, AP rates were up to half those observed in the epipelagic layer, but the fraction < 0.2 µm was not included in the AP measurements (Koike and Nagata, 1997). These authors suggested that the deep-sea AP activity is related to fragmentation and dissolution of rapidly sinking particles. Indeed, it has been shown that the ratios of AP activity determined on particles to the AP activities in bulk seawater were highest among different tested enzymes (Smith et al., 1992). Note, however, that our study sampled only the top of mesopelagic layers (1000 m). Tamburini et al. (2002) obtained a different relative contribution of deep-sea samples when using MUF–P concentrations of 25 nM or 5 µM at the DYFAMED station in the NW Mediterranean Sea (down to 2000 m depth), further showing the artifact of the concentration used. The deep enzymatic activities could be $\times 1.4$ to $\times 2.6$ times higher due to the effect of hydrostatic pressure. Specific AP decreased at five stations and increased at three other stations, and at the two remaining stations, specific Vm_{all} increased, while specific Vm_1 decreased (Fig. 9b). Similarly for the deepest layers sampled (FAST: 2500 m; ION: 3000 m), results also showed no depth trend since specific AP decreased with depth at ION and increased at FAST. The POC / POP ratio did not change with depth. However, the variability in the trend with depth seen for the specific AP activities was also observed in the DOC / DOP ratio. In short, while we expected to see an increase in specific activities with depth due to a preferential removal of P, this was not systematically the case.

LAP activities showed more pronounced trends with depth than AP. Cell-specific LAP showed contradictory results: at all stations cell-specific Vm_1 decreases with depth (according to the DVF criterion; Fig. 9a), whereas Vm_{all} remained stable (2 stations out of 10) or increased with depth (5 stations out of 10). Using a high concentration of MCA-leu, other authors have found an increase in LAP activity per cell with depth in bathypelagic layers (Zaccone et al., 2012; Caruso et al., 2013).

The use of a large concentration set also impacts the Km values because if only a high-concentration range is used, the kinetic contribution of any enzyme with high affinity would be hidden. Baltar et al. (2009b), using a concentration of substrates ranging from 0.6 to 1200 µM, reported an increase in the Km of LAP (from ∼ 400 to 1200 µM) and AP (from ∼ 2 to 23 µM) with depths down to 4500 m in the subtropical Atlantic. In contrast, Tamburini et al. (2002), using a concentration of substrates ranging from 0.05 to 50 µM, obtained lower Km values (ranging between 0.4 and 1.1 µM) for LAP in the Mediterranean deep waters (down to 2000 m depth). It is however difficult to come to a conclusion about the effect of the concentration set tested on Km variability with depth by comparing two studies from different environments and using different sets of substrate concentrations. In our study, where both kinetics were determined in the same waters, among the two parameters Vm and Km, Km showed the largest differences between the two types of kinetics. At many stations (TYR, ION, FAST and ST10), the Km_1 of LAP was stable or decreased with depth, whereas Km_{all} increased, suggesting that within deep layers LAP activity was linked more to the availability of suspended particles or fresh organic matter from sinking material than to DON. Thus, the difference between Km_1 and Km_{all} might reflect adaptive strategies to spatial and/or temporal patchiness in the distribution of suspended particles. Freshly sinking material was probably not present in our incubations because of the small volume of water used but could have contributed to the release of free bacteria, small suspended particles and DOM within its associated plume (Azam and Long, 2001; Tamburini et al., 2003; Grossart et al., 2007; Fang et al., 2015). Baltar et al. (2009a) also suggested that hot spots of activity at depth were associated with particles. The fact that the C/N ratio of particulate material increased with depth (from 11–12 to 22–25) but not so much for DOC / DON (from 13–12 to 14–15 from SURF and DCM to LIW and MDW, respectively) also indicates a preferential utilization of protein substrates from particles. Recently, Zhao et al. (2020) suggested that deep-sea prokaryotes and their metabolism are likely associated with particles rather than DOC based on the increasing contribution of genes encoding secretory enzymes. In contrast to the results for AP, the higher differences between the two LAP enzymatic systems suggest that the microorganisms responsible for the LAP activity face large gradients of protein concentrations and are adapted to pulsed inputs of particles.

4.3 How the set of concentrations used affects interpretation of enzymatic properties as indicators of nutrient imbalance of DOM quality and stoichiometry

In epipelagic waters, both AP maximum rates (Vm_1, Vm_{all}) significantly increased by around 3-fold from the Algerian and Ligurian basins to the Tyrrhenian Basin (t test; $p = 0.002$ and $p = 0.02$, respectively) and reached maximum values at ION. This longitudinal increase was also confirmed by specific activities. This increase in cell-specific AP activities appears to follow a decrease in phosphate availability. While inorganic phosphate can be assimilated directly through a high-affinity absorption pathway, the assimilation of DOP requires its mineralization to free DIP, which is then assimilated. POP is an indicator of living biomass and enzyme producers, but the correlation between Vm AP and POP was negative in the surface layers (log–log relationship; $r = -0.86$ and -0.88 for Vm_{all} and Vm_1, respectively; $p < 0.01$ in both cases), suggesting that the progressive eastward decline in living biomass, and its phosphate availability was accompanied by increased AP expression. Vm in the surface did not correlate with DIP; however the relative DIP deficiency increased eastward, suggested by the deepening of the phosphacline (Table 1), the decrease in average DIP concentrations within the phosphate-depleted layer and the decrease in P diffusive fluxes reaching the surface layer (Pulido-Villena et al., 2021). Along a trans-Mediterranean transect, Zaccone et al. (2012), did not observe a relation between DIP and AP, although they also found increased values of AP-specific activities in the eastern Mediterranean Sea. Bogé et al. (2012), using a concentration set close to ours (0.03–30 µM MUF–P), obtained biphasic kinetics with high differences in the two Vm values (contrary to our results) and described different relationships between Vm and DOP or DIP depending on the low- or high-affinity enzyme. Such differences could be due to the large gradient of trophic conditions in their study, carried out in a eutrophic bay where DOP and DIP concentration ranged from 0 to 185 nM and from 0 to 329 nM, respectively. In contrast, the range of DIP concentrations in our surface water samples was narrow, and values were very low (4–17 nM).

The AP / LAP activity ratio can be used as an indicator of N–P imbalance as demonstrated in enrichment experiments (Sala et al., 2001). In this study using high concentrations of substrates (200 µM), the authors described a decrease in the AP / LAP activity ratio following DIP addition and, conversely, a large increase (10-fold) after the addition of 1 µM nitrate. In their initial experimental conditions, the ratios ranged from 0.2 to 1.9. We observed a similar low ratio in the western Mediterranean Sea, but in the Ionian Sea the AP / LAP activity ratio reached 17 (Vm_{all}) and 43 (Vm_1; Fig. S4a), suggesting that nutrient stresses and imbalances can be as important and variable in different regions of the Mediterranean. Such imbalances are more visible in the high-affinity systems.

LAP / βGLU activity ratio is used as an index of the ability of marine bacteria to preferentially metabolize proteins rather than polysaccharides. Within epipelagic layers, the prevalence of LAP over βGLU is common in temperate areas (Christian and Karl, 1995; Rath et al., 1993) and at high latitudes (Misic et al., 2002, Piontek et al., 2014). The LAP / βGLU activity ratio varied widely from the Equator to

the Southern Ocean, ranging from 0.28 to 593 (Sinsabaugh and Follstad Shah, 2012). In the Ross Sea, this ratio exhibited a relationship with primary production (Misic et al., 2002). In the Caribbean Sea, along a eutrophic-to-oligotrophic gradient, the LAP / βGLU activity ratio increased in oligotrophic conditions (Rath et al., 1993). In the epipelagic zone, during our study, a small westward gradient in productivity (18 to 35 mg TChl a m^{-2}) was found; LAP / βGLU activity ratios ranged from east to west between 3 and 17 for Vm_{all} and from 8 to 34 for Vm_1 (Fig. S4b) and thus varied according to the productivity gradient but also to the concentration set tested, in agreement with previously reported ratios (10 and 20 for the low-concentration and high-concentration range, respectively; Unanue et al., 1999). Finally, the LAP / βGLU activity ratios reported here and in other studies using low substrate ranges are lower than when using higher concentration sets: 20–200 in the subarctic Pacific (Fukuda et al., 2000, using 200 µM concentration) and 213 at the ALOHA station in the equatorial Pacific (Christian and Karl, 1995; using L-leucyl-β-naphthylamine instead of MCA-leu at 1000 µM and MUF–βglu at 1.6 µM), suggesting that the LAP / βGLU activity ratio is highly variable and with a nonlinear dependence on the fluorogenic-substrate concentration. As observed for AP / LAP, the LAP / βGLU activity ratio showed much higher variations for the low-affinity enzyme.

Throughout the water column, variations in the relative activity of different enzymes are also suggested as a possible indicator of changes in bacterioplankton nutrition patterns. The LAP / βGLU activity ratio decreased with depth, following the decrease in the protein-to-carbohydrate ratio of particulate material (Misic et al., 2002) as nitrogen is re-mineralized faster than carbon. However, the TAA-C / TCHO-C ratios were consistently higher within the DCM layer ($\sim$ 90 m) than at the surface, and the LAP / βGLU activity ratio of both Vm_1 and Vm_{all} increased as a consequence, revealing important DON cycling (relative to DOC) at the DCM in comparison to the mixed layers. Below the DCM, the particulate C/N ratio increased with depth, and TAA-C /TCHO-C decreased, likewise indicating a faster hydrolysis of N-rich compounds. We estimated Vm_{all} LAP / Vm_{all} βGLU activity ratios from a few of the single rates measured at high concentration (most βGLU kinetics at depth were not available) and observed, in contrast to Misic et al. (2002), an increase in the ratio within deep layers as βGLU decreased faster than LAP with depth. A bias could be due to the absence of βGLU kinetics at depth; nevertheless other authors have also shown an increase in LAP / βGLU activity ratios with depth (Hoppe and Ullrich, 1999, in the Indian Ocean; Placenti et al., 2018, in the Ionian Sea).

4.4 How the set of concentrations used affects potential contribution of macromolecule hydrolysis to bacterial production

Our results clearly showed the influence of the concentration set used to estimate in situ hydrolysis rates. If the experimentally added substrate concentration is clearly above the possible range of concentrations found in the natural environment, in situ rates could be largely overestimated. To obtain a significant determination of the in situ rates, the added substrate concentrations should be close to the range of variation expected in the studied environment (Tamburini et al., 2002).

We compared the in situ LAP hydrolysis rates to the N demand of heterotrophic prokaryotes (which was based on BP data assuming no active excretion of nitrogen and a C/N ratio of 5). Similarly, the in situ rates of TAAs plus TCHOs were compared to the bacterial carbon demand (based on a bacterial growth efficiency of 10 %; Gazeau et al., 2020; Céa et al., 2014; Lemée et al., 2002). Using the global model, in situ hydrolysis of TAAs by LAP contributed only 25 % $\pm$ 22 % of the bacterial N demand in epipelagic layers and 26 % $\pm$ 24 % in deep layers. This contribution increased using the high-affinity enzyme constants (48 % $\pm$ 29 % and 180 % $\pm$ 154 % in epipelagic layers and deep layers, respectively). In the North Atlantic, the contribution of LAP hydrolysis rates of particles (0.3 µM MCA-leucine added) to bacterial nitrogen demand varied between 63 % and 87 %, increasing at 200 m. Crottereau and Delmas (1998) also computed in situ hydrolysis using combined amino acid concentrations and LAP kinetics and found a range of 6 %–121 % contribution to bacterial N demand in aquatic eutrophic ponds. A large variability in LAP hydrolysis contribution to bacterial N demand has also been detected in coastal estuarine environments using a radio-labeled natural protein as a substrate (2 %–44 %; Keil and Kirchman, 1993). Piontek et al. (2014) used the turnover of βGLU and LAP determined with 1 µM analog substrate concentrations to compute in situ TAA and TCHO hydrolysis rates along a 79° N transect in the North Atlantic and showed that 134 % and 52 % of BP could be supported by peptide and polysaccharides hydrolyzed by enzyme activities, respectively. Based on a bacterial growth efficiency of 10 %, these fluxes will represent 10 times less, i.e., 13 % and 5 % of bacterial carbon demand, which is of the order of magnitude that we obtained. In our study, the contribution of TAA hydrolysis to bacterial N demand was higher in the DCM than in the SURF (10 %–40 % based on the high-affinity enzyme). Nevertheless, this calculation may be biased as marine cyanobacteria such as *Synechococcus* and *Prochlorococcus*, which are dominating phytoplankton groups in the Mediterranean Sea (Siokou-Frangou et al., 2010), can also express LAP (Martinez and Azam, 1993) to satisfy their N requirements. During our study, primary production (PP) peaked in the DCM (Marañón et al., 2021). Size fractionation of primary production showed the importance of phytoplankton excretion, which contributed between 20 %–55 % of the

total PP depending on the station (Marañón et al., 2021). Within the surface mixed layer, other sources of N such as atmospheric deposition could sustain a significant part of bacterial N demand. The dry atmospheric deposition (inorganic) of N at all stations within the PEACETIME cruise corresponded to 27 ± 23 % of bacterial N demand (Van Wambeke et al., 2020).

The in situ cumulated hydrolysis rates of TCHOs by βGLU, estimated only in epipelagic layers, were ~ 3 times higher using the high-affinity enzyme. We summed C sources coming from the hydrolysis by LAP and by βGLU in epipelagic layers (Fig. 11) and compared them to the bacterial carbon demand. Dissolved proteins and combined carbohydrates contributed to only a small fraction of the bacterial carbon demand: 1.5 % based on the low-affinity enzyme and 3 % based on the high-affinity enzyme.

Only within deeper layers were the hydrolysis rates of TAAs at some stations higher than bacterial N demand, suggesting that proteolysis is one of the major sources of N for heterotrophic bacteria in aphotic layers. However, this was only based on the high-affinity enzymes where we found cases of over-hydrolysis of organic nitrogen (Fig. 10). This over-hydrolysis was particularly marked in the LIW of the Tyrrhenian Basin, where over-hydrolysis up to 220 % was obtained as well as higher TAA concentrations in comparison to "older" LIW in the Algerian Basin. TAAs decreased faster than DON along the LIW trajectory, indicating that the labile DON fraction (combined amino acids) was degraded first. Sinking particles or large aggregates associated with attached bacteria are considered to be major providers of labile organic matter for free bacteria (Smith et al., 1992). Within the 5 mL volume of water hydrolyzed for TAA analysis and the 2 mL water volume used to determine ectoenzymatic kinetics, most of this particulate detrital pool is underrepresented, and thus the contribution of TAA hydrolysis to bacterial nitrogen demand is underestimated. However, there is increasing evidence of release from particles not only of monomers issued from hydrolysis but also of ectoenzymes produced by deep-sea prokaryotes attached to particles themselves (Zhao et al., 2020). This could explain why, in our small volumes, we still observe multiple kinetics. Studying alkaline phosphatase activity in the Toulon Bay, Bogé et al. (2013) observed biphasic kinetics only in the dissolved phase, which also suggests that low-affinity AP originates from enzyme secretion by prokaryotes attached to particles. Further, the study of size-fractionated particulate material showed that the origin of the low-affinity enzymes was mostly within the > 90 µm fraction (Bogé et al., 2017).

5 Conclusions

Vertical and regional variability in enzyme activities were found in the Mediterranean Sea, where heterotrophic prokaryotes face not only carbon but also N and P limitations. Although biased by the use of artificial fluorogenic substrates, ectoenzymatic activity is an appropriate tool to study the adaptation of prokaryotes to the environmental gradients in stoichiometry, chemical characteristics and organic matter concentrations. We have shown that the relative increase or decrease in Vm or specific activities per depth is largely related to the choice of concentration set used in the kinetic measurements. The activity ratios of AP / LAP or LAP / βGLU used to track nutrient imbalances in the DOM pool showed a larger range of variation in low-affinity enzymes. Finally, to obtain robust determination of in situ enzymatic rates, the added substrate concentrations should be close to the range of variation expected in the studied area. While the use of the microplate titration technique greatly improved the simultaneous study of different enzymes, assessments of enzyme kinetics should be performed systematically in enzymatic studies. Future combination of such techniques with the chemical identification of DOC and DON pools and meta-omics as well as the use of marine snow catchers will help our understanding of the biodegradation of organic matter in the ocean.

Data availability. Underlying research data are being used by researcher participants of the PEACETIME campaign to prepare other papers, and therefore data are not publicly accessible at the time of publication. "Biogeochemical dataset collected during the PEACETIME cruise" (Guieu et al., 2020a) will be accessible at https://www.seanoe.org/data/00645/75747/ (Guieu et al., 2020b) once the special issue is completed (all papers should be published by June 2021).

Supplement. The supplement related to this article is available online at: https://doi.org/10.5194/bg-18-2301-2021-supplement.

Author contributions. FVW and CT designed the study. FVW, CT, MG and SG sampled and incubated samples for ectoenzymatic activity on board; FVW and SG analyzed the ectoenzymatic data. FVW and MG sampled and analyzed BP samples, BZ sampled and analyzed TAA and TCHO samples, AE managed the TCHO and TAA analysis and treatments, EP and KD sampled and analyzed DIP with the LWCC technique, SN sampled and analyzed nutrients and organic matter, VT assisted in CTD operations and analyzed water masses, JD sampled for DOC and flow cytometry, PC analyzed bacterial abundances, BM analyzed DOC, and FVW prepared the paper with contributions from all co-authors.

Competing interests. The authors declare that they have no conflict of interest.

Special issue statement. This article is part of the special issue "Atmospheric deposition in the low-nutrient–low-chlorophyll (LNLC)

ocean: effects on marine life today and in the future (ACP/BG inter-journal SI)". It is not associated with a conference.

Acknowledgements. The authors thank many scientists and engineers for their assistance with sampling and analyses: Jon Roa for TCHOs, Ruth Flerus for TAA, Joris Guittoneau for nutrients, Thierry Blasco for POC, Julia Uitz and Céline Dimier for Chl *a* (analyzed at the SAPIGH HPLC analytical service at the IMEV, Villefranche), Ingrid Obernosterer for DOC. We warmly thank Cécile Guieu and Karine Deboeufs as coordinators of the program PEACETIME and chief scientists of the cruise. We are grateful to the two anonymous reviewers and the editor Christine Klass for their constructive and pertinent comments. This study is a contribution to the PEACETIME project (http://peacetime-project.org, last access: 30 March 2021), a joint initiative of the MERMEX and ChArMEx components. The PEACETIME cruise was endorsed as a process study by GEOTRACES and is also a contribution to IMBER and SOLAS.

Financial support. The project leading to this publication has received funding from CNRS-INSU, IFREMER, CEA, and Météo-France as part of the programme MISTRALS coordinated by INSU (https://doi.org/10.17600/17000300) and from the European FEDER fund under project no. 1166-39417. The publication of this article is financed by CNRS-INSU.

Review statement. This paper was edited by Christine Klaas and reviewed by two anonymous referees.

References

Aluwihare, L. I., Repeta, D. J., and Chen, R. F.: A major biopolymeric component to dissolved organic carbon in surface sea water, Nature, 387, 166–169, https://doi.org/10.1038/387166a0, 1997.

Aminot, A. and Kérouel, R.: Dosage automatique des nutriments dans les eaux marines, in: Méthodes d'analyses en milieu marin, Ifremer, Plouzané, 188, IBSN no. 978-2-7592-0023-8, 2007.

Arnosti, C.: Microbial Extracellular enzymes and the marine carbon cycle, Annu. Rev. Mar. Sci., 3, 401–425, 2011.

Arrieta, J. M. and Herndl, G. J.: Assessing the diversity of marine bacterial β-glucosidases by capillary Electrophoresis Zymography, Appl. Environ. Microb., 67, 4896–4900, 2001.

Azam, F. and Long, R. A.: Sea snow microcosms, Nature, 414, 495–498, 2001.

Azzaro, M., La Ferla, R., Maimone, G., Monticelli, L. S., Zaccone, R., and Civitarese, G.: Prokaryotic dynamics and heterotrophic metabolism in a deep convection site of Eastern Mediterranean Sea (the Southern Adriatic Pit), Cont. Shelf Res., 44, 106–118, https://doi.org/10.1016/j.csr.2011.07.011, 2012.

Baltar, F.: Watch Out for the "Living Dead": Cell-Free Enzymes and Their Fate, Front. Microbiol., 8, 2438, https://doi.org/10.3389/fmicb.2017.02438, 2018.

Baltar, F., Arístegui, J., Gasol, J. M., Sintes, E., and Herndl, G. J.: Evidence of prokaryotic metabolism on suspended particulate organic matter in the dark waters of the subtropical North Atlantic, Limnol. Oceanogr., 54, 182–193, https://doi.org/10.4319/lo.2009.54.1.0182, 2009a.

Baltar, F., Arístegui, J., Sintes, E., van Aken, H. M., Gasol, J. M., and Herndl, G. J.: Prokaryotic extracellular enzymatic activity in relation to biomass production and respiration in the meso- and bathypelagic waters of the (sub)tropical Atlantic, Environ. Microbiol., 11, 1998–2014, 2009b.

Bogé, G., Lespilette, M., Jamet, D., and Jamet, J.-L.: Role of sea water DIP and DOP in controlling bulk alkaline phosphatase activity in N.W. Mediterranean Sea (Toulon, France), Mar. Pollut. Bull., 64, 1989–1996, https://doi.org/10.1016/j.marpolbul.2012.07.028, 2012.

Bogé, G., Lespilette, M., Jamet, D., and Jamet, J.-L.: The relationships between particulate and soluble alkaline phosphatase activities and the concentration of phosphorus dissolved in the seawater of Toulon Bay (NW Mediterranean), Mar. Pollut. Bull., 74, 413–419, https://doi.org/10.1016/j.marpolbul.2013.06.003, 2013.

Bogé, G., Lespilette, M., Jamet, D., and Jamet, J.-L.: Role of DOP on the alkaline phosphatase activity of size fractionated plankton in coastal waters in the NW Mediterranean Sea (Toulon Bay, France), Mar. Pollut. Bull., 117, 264–273, https://doi.org/10.1016/j.marpolbul.2016.11.037, 2017.

Caruso, G., Monticelli, L., La Ferla, R., Maimone, G., Azzaro, M., Azzaro, F., Decembrini, F., De Pasquale, F., Leonardi, M., Raffa, F., Zappal, G., and De Domenico, E.: Patterns of Prokaryotic Activities and Abundance among the Epi-Meso and Bathypelagic Zones of the Southern-Central Tyrrhenian Sea, Oceanography, 1, 1000105, https://doi.org/10.4172/ocn.1000105, 2013.

Cauwet, G.: Determination of dissolved organic carbon (DOC) and nitrogen (DON) by high temperature combustion, in: Methods of Seawater analysis, edited by: Grashoff, K., Kremling, K., and Ehrhard, M., edn. 3, Wiley-VCH Verlag, Weinheim, Baden-Württemberg, Germany, 407–420, 1999.

Céa, B., Lefèvre, D., Chirurgien, L., Raimbault, P., Garcia, N., Charrière, B., Grégori, G., Ghiglione, J.-F., Barani, A., Lafont, M., and Van Wambeke, F.: An annual survey of bacterial production, respiration and ectoenzyme activity in coastal NW Mediterranean waters: temperature and resource controls, Environ. Sci. Pollut. R., 22, 13654–13668, https://doi.org/10.1007/s11356-014-3500-9, 2014.

Christian, J. R. and Karl, D. M.: Bacterial ectoenzymes in marine waters: Activity ratio and temperature responses in three oceanographic provinces, Limnol. Oceanogr., 40, 1046–1053, 1995.

Chróst, R. J.: Microbial enzymes in aquatic environments, Springer-Verlag, New York, USA, 1991.

Crottereau, C. and Delmas, D.: Exoproteolytic activity in an Atlantic pond (France): estimates of in situ activity, Aquat. Microb. Ecol., 15, 217–224, 1998.

Dittmar, T. H., Cherrier, J., and Ludwichowski, K.-U: The analysis of amino acids in seawater, in: Practical Guidelines for the Analysis of Seawater, edited by: Wurl, O., CRC-Press, Boca Raton, Florida, USA, 67–78, 2009.

Engel, A. and Händel, N.: A novel protocol for determining the concentration and composition of sugars in particulate and in high molecular weight dissolved organic matter (HMW-DOM) in seawater, Mar. Chem., 127, 180–191, 2011.

Fang, J., Zhang, L., Li, J., Kato, C., Tamburini, C., Zhang, Y., Dang, H., Wang, G., and Wang, F.: The POM-DOM piezophilic microorganism continuum (PDPMC) – The role of piezophilic microorganisms in the global ocean carbon cycle, Sci. China Earth Sci., 58, 106–115, https://doi.org/10.1007/s11430-014-4985-2, 2015.

Fukuda, R., Sohrin, Y., Saotome, N., Fukuda, H., Nagata, T., and Koike, I.: East-west gradient in ectoenzyme activity in the subartic Pacific: Possible regulation by zinc, Limnol. Oceanogr., 45, 930–939, 2000.

Gazeau, F., Ridame, C., Van Wambeke, F., Alliouane, S., Stolpe, C., Irisson, J.-O., Marro, S., Grisoni, J.-M., De Liège, G., Nunige, S., Djaoudi, K., Pulido-Villena, E., Dinasquet, J., Obernosterer, I., Catala, P., and Guieu, C.: Impact of dust enrichment on Mediterranean plankton communities under present and future conditions of pH and temperature: an experimental overview, Biogeosciences Discuss. [preprint], https://doi.org/10.5194/bg-2020-202, in review, 2020.

Grossart, H.-P., Tang, K. W., Kiørboe, T., and Ploug, H.: Comparison of cell-specific activity between free-living and attached bacteria using isolates and natural assemblages, FEMS Microbiol. Lett., 266, 194–200, https://doi.org/10.1111/j.1574-6968.2006.00520.x, 2007.

Guieu, C., and Desboeufs, K. : PEACETIME cruise, RV Pourquoi pas?, https://doi.org/10.17600/17000300, 2017.

Guieu, C., D'Ortenzio, F., Dulac, F., Taillandier, V., Doglioli, A., Petrenko, A., Barrillon, S., Mallet, M., Nabat, P., and Desboeufs, K.: Introduction: Process studies at the air–sea interface after atmospheric deposition in the Mediterranean Sea – objectives and strategy of the PEACETIME oceanographic campaign (May–June 2017), Biogeosciences, 17, 5563–5585, https://doi.org/10.5194/bg-17-5563-2020, 2020a.

Guieu C., Desboeufs, K., Albani, S., et al.: Biogeochemical dataset collected during the PEACETIME cruise, https://www.seanoe.org/data/00645/75747/ (last access: 7 April 2021), 2020b.

Guyennon, A., Baklouti, M., Diaz, F., Palmieri, J., Beuvier, J., Lebaupin-Brossier, C., Arsouze, T., Béranger, K., Dutay, J.-C., and Moutin, T.: New insights into the organic carbon export in the Mediterranean Sea from 3-D modeling, Biogeosciences, 12, 7025–7046, https://doi.org/10.5194/bg-12-7025-2015, 2015.

Hopkins, T. S.: Physical processes in the Mediterranean Basin, in: Estuarine transport processes, edited by: Kjerfve, B., University of South Carolina, South Carolina, USA, 269–310, 1978.

Hoppe, H.-G.: Significance of exoenzymatic activities in the ecology of brackish water: measurements by means of methylumbelliferyl-substrates, Mar. Ecol. Prog. Ser., 11, 299–308, 1983.

Hoppe, H.-G. and Ullrich, S.: Profiles of ectoenzymes in the Indian Ocean: phenomena of phosphatase activity in the mesopelagic zone, Aquat. Microb. Ecol., 19, 139–148, 1999.

Hoppe, H.-G., Ducklow, H., and Karrasch, B.: Evidence for dependency of bacterial growth on enzymatic hydrolysis of particulate organic matter in the mesopelagic ocean, Mar. Ecol. Prog. Ser., 93, 277–283, 1993.

Keil, R. G. and Kirchman, D.: Dissolved combined amino acids: Chemical form and utilization by marine bacteria, Limnol. Oceanogr., 38, 1256–1270, 1993.

Kirchman, D. L.: Leucine incorporation as a measure of biomass production by heterotrophic bacteria, in: Handbook of methods in aquatic microbial ecology, edited by: Kemp, P. F., Sherr, B. F., Sherr, E. B., and Cole, J. J., Lewis, Boca Raton, Florida, USA, 509–512, 1993.

Koch, A. L.: Oligotrophs versus copiotrophs, BioEssays, 23, 657–661, 2001.

Koike, I. and Nagata, T.: High potential activity of extracellular alkaline phosphatase in deep waters of the central Pacific, Deep-Sea Res. Pt. II, 44, 2283–2294, 1997.

Kress, N., Manca, B., Klein, B., and Deponte, D.: Continuing influence of the changed thermohaline circulation in the eastern Mediterranean on the distribution of dissolved oxygen and nutrients: Physical and chemical characterization of the water masses, J. Geophys. Res.-Oceans, 108, 8109, https://doi.org/10.1029/2002JC001397, 2003.

Krom, M. D., Herut, B., and Mantoura, R. F. C.: Nutrient budget for the eastern Mediterranean: Implication for phosphorus limitation, Limnol. Oceanogr, 49, 1582–1592, https://doi.org/10.4319/lo.2004.49.5.1582, 2004.

Lascaratos, A., Roether, W., Nittis, K., and Klein, B.: Recent changes in deep water formation and spreading in the eastern Mediterranean Sea: a review, Prog. Oceanogr., 44, 5–36, 1999.

Lemée, R., Rochelle-Newall, E., Van Wambeke, F., Pizay, M.-D., Rinaldi, P., and Gattuso, J.-P.: Seasonal variation of bacterial production, respiration and growth efficiency in the open NW Mediterranean Sea, Aquat. Microb. Ecol., 29, 227–237, 2002.

Lindroth, P. and Mopper, K.: High performance liquid chromatographic determination of subpicomole amounts of amino acids by precolumn fluorescence derivatization with o-phthaldialdehyde, Anal. Chem., 51, 1667–1674, 1979.

Malanotte-Rizzoli, P., Manca, B. B., Marullo, S., Ribera d'Alcalà, M., Roether, W., Theocharis, A., and Conversano, F.: The Levantine Intermediate Water Experiment (LIWEX) Group: Levantine basin – A laboratory for multiple water mass formation processes, J. Geophys. Res.-Oceans, 108, 8101, https://doi.org/10.1029/2002JC001643, 2003.

Marañón, E., Van Wambeke, F., Uitz, J., Boss, E. S., Dimier, C., Dinasquet, J., Engel, A., Haëntjens, N., Pérez-Lorenzo, M., Taillandier, V., and Zäncker, B.: Deep maxima of phytoplankton biomass, primary production and bacterial production in the Mediterranean Sea, Biogeosciences, 18, 1749–1767, https://doi.org/10.5194/bg-18-1749-2021, 2021.

Martinez, J. and Azam, F.: Aminopeptidase activity in marine chroococcoid cyanobacteria, Appl. Environ. Microb., 59, 3701–3707, 1993.

Martinez, J., Smith, D. C., Steward, G. F., and Azam, F.: Variability in ectohydrolytic enzyme activities of pelagic marine bacteria and its significance for substrate processing in the sea, Aquat. Microb. Ecol., 10, 223–230, 1996.

Misic, C., Povero, P., and Fabiano, M.: Ectoenzymatic ratios in relation to particulate organic matter distribution (Ross Sea, Antarctica), Microbial Ecol., 44, 224–234, https://doi.org/10.1007/s00248-002-2017-9, 2002.

Piontek, J., Sperling, M., Nothig, E.-V., and Engel, A.: Regulation of bacterioplankton activity in Fram Strait (Arctic Ocean) during early summer: The role of organic matter supply and temperature, J. Marine Syst., 132, 83–94, https://doi.org/10.1016/j.jmarsys.2014.01.003, 2014.

Placenti, F., Azzaro, M., Artale, V., La Ferla, R., Caruso, G., Santinelli, C., Maimone, G., Monticelli, L. S., Quinci, E. M., and

Sprovieri, M.: Biogeochemical patterns and microbial processes in the Eastern Mediterranean Deep Water of Ionian Sea, Hydrobiologia, 815, 97–112, https://doi.org/10.1007/s10750-018-3554-7, 2018.

Pulido-Villena, E., Djaoudi, K., Desboeufs, K., Van Wambeke, F., Barrillon, S., Doglioli, A., Petrenko, A., Taillandier, V., D'Ortenzio, F., Fu, F., Gaillard, T., Guasco, S., Nunige, S., Triquet, S., and Guieu, C.: Phosphorus cycling in the upper waters of the Mediterranean Sea (Peacetime cruise): relative contribution of external and internal sources, in preparation for Biogeosciences, 2021, special issue PEACETIME.

Raimbault, P., Pouvesle, W., Diaz, F., Garcia, N., and Sempere, R.: Wet-oxidation and automated 930 colorimetry for simultaneous determination of organic carbon, nitrogen and phosphorus dissolved in seawater, Mar. Chem., 66, 161–169, 1999.

Rath, J., Schiller, C., and Herndl, G. J.: Ectoenzyme activity and bacterial dynamics along a trophic gradient in the Caribbean Sea, Mar. Ecol. Prog. Ser., 102, 89–96, 1993.

Sala, M. M., Karner, M., Arin, L., and Marrassé, C.: Measurement of ectoenzyme activities as an indication of inorganic nutrient imbalance in microbial communities, Aquat. Microb. Ecol., 23, 301–311, https://doi.org/10.3354/ame023301, 2001.

Schroeder, K., Cozzi, S., Belgacem, M., Borghini, M., Cantoni, C., Durante, S., Petrizzo, A., Poiana, A., and Chiggiato, J.: Along-Path Evolution of Biogeochemical and Carbonate System Properties in the Intermediate Water of the Western Mediterranean, Front. Mar. Sci., 7, 375, https://doi.org/10.3389/fmars.2020.00375, 2020.

Severin, T., Sauret, C., Boutrif, M., Duhaut, T., Kessouri, F., Oriol, L., Caparros, J., Pujo-Pay, M., Durrieu de Madron, X., Garel, M., Tamburini, C., Conan, P., and Ghiglione, J. F.: Impact of an intense water column mixing (0–1500 m) on prokaryotic diversity and activities during an open-ocean convection event in the NW Mediterranean Sea, Environ. Microbiol., 18, 4378–4390, https://doi.org/10.1111/1462-2920.13324, 2016.

Sharp, J. H.: Improved analysis for "particulate" organic carbon and nitrogen from seawater, Limnol. Oceanogr., 19, 984–989, 1974.

Simon, M., Grossart, H., Schweitzer, B., and Ploug, H.: Microbial ecology of organic aggregates in aquatic ecosystems, Aquat. Microb. Ecol., 28, 175–211, https://doi.org/10.3354/ame028175, 2002.

Sinsabaugh, R. and Follstad Shah, J.: Ectoenzymatic Stoichiometry and Ecological Theory, Annu. Rev. Ecol. Evol. S., 43, 313–343, https://doi.org/10.1146/annurev-ecolsys-071112-124414, 2012.

Siokou-Frangou, I., Christaki, U., Mazzocchi, M. G., Montresor, M., Ribera d'Alcalá, M., Vaqué, D., and Zingone, A.: Plankton in the open Mediterranean Sea: a review, Biogeosciences, 7, 1543–1586, https://doi.org/10.5194/bg-7-1543-2010, 2010.

Smith, D. C. and Azam, F.: A simple, economical method for measuring bacterial protein synthesis rates in sea water using 3H-Leucine, Marine Microbial Food Webs, 6, 107–114, 1992.

Smith, D. C., Simon, M., Alldredge, A. L., and Azam, F.: Intense hydrolytic activity on marine aggregates and implications for rapid particle dissolution, Nature, 359, 139–142, 1992.

Stocker, R.: Marine Microbes See a Sea of gradients, Science, 38, 628–633, 2012.

Taillandier, V., Prieur, L., D'Ortenzio, F., Ribera d'Alcalà, M., and Pulido-Villena, E.: Profiling float observation of thermohaline staircases in the western Mediterranean Sea and impact on nutrient fluxes, Biogeosciences, 17, 3343–3366, https://doi.org/10.5194/bg-17-3343-2020, 2020.

Tamburini, C., Garcin, J., Ragot, M., and Bianchi, A.: Biopolymer hydrolysis and bacterial production under ambient hydrostatic pressure through a 2000 m water column in the NW Mediterranean, Deep-Sea Res. Pt. II, 49, 2109–2123, https://doi.org/10.1016/S0967-0645(02)00030-9, 2002.

Tamburini, C., Garcin, J., and Bianchi, A.: Role of deep-sea bacteria in organic matter mineralization and adaptation to hydrostatic pressure conditions in the NW Mediterranean Sea, Aquat. Microb. Ecol., 32, 209–218, https://doi.org/10.3354/ame032209, 2003.

Tamburini, C., Garel, M., Al Ali, B., Mérigot, B., Kriwy, P., Charrière, B., and Budillon, G.: Distribution and activity of Bacteria and Archaea in the different water masses of the Tyrrhenian Sea, Deep-Sea Res. Pt. II, 56, 700–714, https://doi.org/10.1016/j.dsr2.2008.07.021, 2009.

Testor, P., Bosse, A., Houpert, L., Margirier, F., Mortier, L., Legoff, H., Dausse, D., Labaste, M., Kartensen, J., Hayes, D., Olita, A., Ribotti, A., Schroeder, K., Chiggiato, J., Onken, R., Heslop, R., Mourre, B., D'Ortenzio, F., Mayot, N., Lavigne, H., de Fommervault, O., Coppola, L., Prieur, L., Taillandier, V., Durrieu de Madron, X., Bourrin, F., Many, G., Damien, P., Estournel, C., Marsaleix, P., Taupier-Lepage, I., Raimbault, P., Waldman, R., Bouin, M.-N., Giordani, H., Caniaux, G., Somot, S., Ducrocq, V., and Conan, P.: Multiscale observations of deep convection in the northwestern Mediterranean Sea during winter 2012–2013 using multiple platforms, J. Geophys. Res.-Oceans, 123, 1745–1776, https://doi.org/10.1002/2016JC012671, 2018.

The Mermex Group: Marine ecosystems' responses to climatic and anthropogenic forcings in the Mediterranean, Prog. Oceanogr., 91, 97–166, https://doi.org/10.1016/j.pocean.2011.02.003, 2011.

Thingstad, T. F. and Rassoulzadegan, F.: Nutrient limitations, microbial food webs, and "biological C-pumps": suggested interactions in a P-limited Mediterranean, Mar. Ecol. Prog. Ser., 117, 299–306, 1995.

Tholosan, O., Lamy, F., Garcin, J., Polychronaki, T., and Bianchi, A.: Biphasic extracellular proteolytic enzyme activity in benthic water and sediment in the North Western Mediterranean Sea, Appl. Environ. Microb., 65, 1619–1626, 1999.

Unanue, M., Ayo, B., Agis, M., Slezak, D., Herndl, G. J., and Iriberri, J.: Ectoenzymatic activity and uptake of monomers in marine bacterioplankton described by a biphasic kinetic model, Microbial Ecol., 37, 36–48, https://doi.org/10.1007/s002489900128, 1999.

Van Wambeke, F., Christaki, U., Giannakourou, A., Moutin, T., and Souvemerzoglou, K.: Longitudinal and vertical trends of bacterial limitation by phosphorus and carbon in the Mediterranean Sea, Microbial Ecol., 43, 119–133, https://doi.org/10.1007/s00248-001-0038-4, 2002.

Van Wambeke, F., Taillandier, V., Deboeufs, K., Pulido-Villena, E., Dinasquet, J., Engel, A., Marañón, E., Ridame, C., and Guieu, C.: Influence of atmospheric deposition on biogeochemical cycles in an oligotrophic ocean system, Biogeosciences Discuss. [preprint], https://doi.org/10.5194/bg-2020-411, in review, 2020.

Wright, R. T. and Hobbie, J. E.: Use of glucose and acetate by bacteria and algae in aquatic ecosystems, Ecology, 47, 447–464, 1966.

Wust, G.: On the vertical circulation of the Mediterranean Sea, J. Geophys. Res., 66, 3261–3271, 1961.

Zaccone, R. and Caruso, G.: Microbial enzymes in the Mediterranean Sea: relationship with climate changes, AIMS Microbiology, 5, 251–272, 2019.

Zaccone, R., Boldrin, A., Caruso, G., La Ferla, R., Maimone, G., Santinelli, C., and Turchetto, M.: Enzymatic Activities and Prokaryotic Abundance in Relation to Organic Matter along a West–East Mediterranean Transect (TRANSMED Cruise), Microbial Ecol., 64, 54–66, 2012.

Zhang, J.-Z. and Chi, J.: Automated analysis of nano-molar concentrations of phosphate in natural waters with liquid waveguide, Environ. Sci. Technol., 36, 1048–1053, https://doi.org/10.1021/es011094v, 2002.

Zhao, Z., Baltar, B., and Herndl, G. J.: Linking extracellular enzymes to phylogeny indicates a predominantly particle-associated lifestyle of deep-sea prokaryotes, Sciences Advances, 6, eaaz4354, https://doi.org/10.1126/sciadv.aaz4354, 2020.